Ecotoxicology and Environmental Safety 213 (2021) 112041

Contents lists available at ScienceDirect

Ecotoxicology and Environmental Safety

journal homepage: www.elsevier.com/locate/ecoenv

Combined cytotoxicity of polystyrene nanoplastics and phthalate esters on human lung epithelial A549 cells and its mechanism

Qingying Shi [a], Jingchun Tang [a,*], Lan Wang [a], Rutao Liu [b], John P. Giesy [c,d,e]

[a] Key Laboratory of Pollution Processes and Environmental Criteria (Ministry of Education), Tianjin Engineering Center of Environmental Diagnosis and Contamination Remediation, College of Environmental Science and Engineering, Nankai University, Tianjin 300350, China
[b] School of Environmental Science and Engineering, Shandong University, China-America CRC for Environment & Health, 72# Jimo Binhai Road, Qingdao, Shandong 266237, China
[c] Toxicology Centre, University of Saskatchewan, 44 Campus Drive, Saskatoon, SK S7N 5B3, Canada
[d] Dept. Veterinary Biomedical Sciences, University of Saskatchewan, 52 Campus Drive, Saskatoon, SK S7N 5B4, Canada
[e] Dept. Environmental Sciences, Baylor University, Waco, TX 76798-7266, USA

ARTICLE INFO

Edited by Dr Fernando Barbosa

Keywords:
PAEs
Combined cytotoxicity
Bioavailability
Inhalation exposure
Inflammation
Oxidative stress

ABSTRACT

Awareness of risks posed by widespread presence of nanoplastics (NPs) and bioavailability and potential to interact with organic pollutants has been increasing. Inhalation is one of the more important pathways of exposure of humans to NPs. In this study, combined toxicity of concentrations of polystyrene NPs and various phthalate esters (PAEs), some of the most common plasticizers, including dibutyl phthalate (DBP) and di-(2-ethyl hexyl) phthalate (DEHP) on human lung epithelial A549 cells were investigated. When co-exposed, 20 μg NPs/mL increased viabilities of cells exposed to either DBP or DEHP and the modulation of toxic potency of DEHP was greater than that of DBP, while the 200 μg NPs/mL resulted in lesser viability of cells. PAEs sorbed to NPs decreased free phase concentrations (C_{free}) of PAEs, which resulted in a corresponding lesser bioavailability and joint toxicity at the lesser concentration of NPs. The opposite effect was observed at the greater concentration of NPs, which may result from the dominated role of NPs in the combined toxicity. Furthermore, our data showed that oxidative stress and inflammatory reactions were mechanisms for combined cytotoxicities of PAEs and NPs on A549 cells. Results of this study emphasized the combined toxic effects and mechanisms on human lung cells, which are helpful for assessing the risk of the co-exposure of NPs and organic contaminants in humans.

1. Introduction

Microplastics (MPs), having diameters <5 mm, have recently been receiving attention (Besseling et al., 2013; Bouwmeester et al., 2015; Lehner et al., 2019). Further studies indicated that plastic microparticles could be fragmented to form nanoplastics (NPs) (Bouwmeester et al., 2015). These NPs, fragmented from larger plastic particles are classified as secondary NPs (Bouwmeester et al., 2015; Lehner et al., 2019). Primary NPs are also purposely produced, for use in various fields (Dekkers et al., 2011; Forte et al., 2016). As a result, there might be accumulation of NPs in the environment (Forte et al., 2016). NPs have small size and large specific surface area so that organic contaminants can be associated with NPs and penetrate organs of organisms where NPs and associated contaminants can affect biological functions (Bouwmeester et al., 2015; Xu et al., 2019).

Toxic effects of NPs have been extensively studied in aquatic organisms and aquatic environments (Chae and An, 2017; Rios Mendoza et al., 2018). Thereinto, there were a large number of studies available in the literature that investigated the toxic effects of NPs on marine organisms [e.g., arthropods (Zhang et al., 2020), bivalves (Baudrimont et al., 2020), bacteria (Sun et al., 2018), algae (Bhargava et al., 2018), rotifers (Manfra et al., 2017), echinoderms (Della Torre et al., 2014) and fish (Brun et al., 2019)], and several researches in the toxic effects of NPs on freshwater organisms have also been performed [e.g., algae (Nolte et al., 2017), microcrustaceans (Cui et al., 2017) and fish (Estrela et al., 2021; Guimarães et al., 2021a, 2021b)]. However, since they are increasingly accumulating in all compartments of the environment, it is possible for NPs to be accumulated and for humans to be exposed. NPs with sizes ranging from 50 nm to 100 nm can be internalized by human colon adenocarcinoma Caco-2 cells, and cytotoxicity, reactive oxygen

* Corresponding author.
E-mail address: tangjch@nankai.edu.cn (J. Tang).

https://doi.org/10.1016/j.ecoenv.2021.112041
Received 25 November 2020; Received in revised form 5 February 2021; Accepted 6 February 2021
Available online 15 February 2021

species (ROS) increase, genotoxicity, DNA oxidative damage and increases in expressions of genes involved in responses to stress were observed (Cortés et al., 2020). NPs can affect survival and morphologies of cells and expressions of inflammatory factors (Forte et al., 2016). However, there is little information available on toxic potencies of NPs toward cells of humans or wildlife (Bouwmeester et al., 2015; Poma et al., 2019).

For humans, exposure to NPs via inhalation is one of the most important pathways (Lehner et al., 2019). Particles of plastic are widely found in the atmosphere (Xu et al., 2019). Microplastic fibers have been observed in lungs of humans (Dris et al., 2017). Particles of plastic can enter deep lungs and further interact with lung fluid and lung cells, which can subsequently trigger inflammatory responses, which can result in acute and chronic respiratory diseases (Dong et al., 2020).

Phthalate esters (PAEs) are abundant as some of the most used plasticizers to increase flexibility and toughness of polymers (Fred-Ahmadu et al., 2020). They can migrate from greater molecular mass carbon chains and contaminate various environmental media and are ubiquitous in water (Clara et al., 2010; Wu et al., 2017), air (Teil et al., 2006) and soils (Müller and Kördel, 1993). PAEs can cause cytotoxicity, such as DNA damage, oxidative stress, apoptosis and estrogenic effects (Kim et al., 2019), so that they have been considered priority pollutants (Liu et al., 2019a). Di-(2-ethylhexyl) phthalate (DEHP), a kind of PAEs, has been reported to cause cytotoxicity in various types of cells (Erkekoğlu et al., 2010; Molino et al., 2019; Peropadre et al., 2015). For example, DEHP caused significant decreases in cell viability and impaired antioxidant systems and damaged DNA (Erkekoğlu et al., 2010). Another PAE, dibutyl phthalate (DBP) can also cause cytotoxicity (Chen and Chien, 2014; Yu et al., 2009). In addition, Benson and Fred-Ahmadu (2020) indicated that DEHP and DBP were the most dominant PAEs in the investigation of microplastics-sorbed PAEs in littoral sandflat sediments of the Gulf of Guinea.

Although plastic particles and PAEs coexist extensively in various compartments of the environment, their combined toxic effects to organisms are largely unknown (Li et al., 2020a), with even less known about co-toxicity on human health. Due to large specific surface area and inherent hydrophobicity, persistent organic pollutants such as PAEs can be adsorbed on surfaces of plastic particles (Liu et al., 2019a; Shen et al., 2019). Systematic researches of combined toxic effects should be conducted to explore the potential health impacts and risks on human. Combined effects of polystyrene MPs and DBP have been observed on the microalgae, *Chlorella pyrenoidosa*, which demonstrated combined effects of MPs and DBP was variable at different concentration ranges, and MPs could reduce bioavailability of DBP (Li et al., 2020a). Effects of polystyrene NPs on *Ctenopharyngodon idella* (grass carp) after individual and combined exposure with zinc oxide nanoparticles have been detected (Estrela et al., 2021).

In this study, effects of combinations of polystyrene NPs with diameters of 100 nm and two selected PAEs, DEHP and DBP, on a representative human lung epithelial cell line, A549 cells were determined. Thus, the aim of the current study was to test the hypothesis that the human lung epithelial A549 cells exposed to both NPs and PAEs (DEHP and DBP) may present changes in cell viability, oxidative stress and inflammatory reaction due to the interaction of NPs and PAEs, and these changes may vary depending on the concentrations of NPs and the properties of PAEs. This is the first time such interactions have been evaluated to inform assessments of risks to the human respiratory system caused by co-exposure of NPs and PAEs.

2. Material and methods

2.1. Materials

Unmodified polystyrene NPs and green fluorescent polystyrene NPs of 100 nm diameter were obtained from Huge Biotechnology Co., Ltd. (Shanghai, China; density 1.05 g/cm^3; Product n. DS100). Methanol (purity >99.9%; CAS number 67–56–1) was purchased from J&K Chemicals Ltd. (Shanghai, China). DEHP (purity >99%; CAS number 117–81–7) and DBP (purity >99%; CAS number 84–74–2) dissolved in methanol were purchased from Aladdin Bio-Chem Technology Co., Ltd. (Shanghai, China) (Table S1), and the stock solutions of DEHP and DBP of 50 mg/mL were prepared in methanol and stored at 4 °C and protected from direct light. To minimize the co-solvent effect and avoid toxicity, concentrations of methanol in test solutions were less than 0.01%. Human alveolar type II epithelial cell line, A549, was purchased from Shanghai Institute of Biochemistry and Cell Biology (Shanghai, China). RPMI-1640 medium was purchased from Gibco (ThermoFisher, Carlsbad, California, US; Product n. C11875500BT). Fetal bovine serum (FBS) from Biological Industries (Israel; Product n. 04–001–1ACS) were used to culture A549 cells. Penicillin-Streptomycin solution (Product n. 10378016) and trypsin-ethylenediamine tetra-acetic acid (Trypsin-EDTA) buffer were purchased from Gibco (ThermoFisher, Carlsbad, California, US; Product n. 25200072). Cell Counting Kit-8 (CCK-8; Product n. C0038) and ROS assay kits (DCFH-DA, Product n. S0033S) were purchased from Beyotime Biotechnology Co., Ltd. (Shanghai, China). Assay kits for superoxide dismutase (SOD; Product n. S0101S), catalase (CAT; Product n. S0051), glutathione peroxidase (GSH-Px; Product n. S0056) and malondialdehyde (MDA; Product n. S0131S) were purchased from Beyotime Biotechnology Co., Ltd. (Shanghai, China). Bicinchoninic acid (BCA) protein assay kit was purchased from Beijing Solarbio Science & Technology Co., Ltd. (Beijing, China; Product n. PC0020). 4′,6-diamidino-2-phenylindole (DAPI) were purchased from Beyotime Biotechnology Co., Ltd. (Shanghai, China; Product n. C1005). RNAiso Plus reagent was acquired from Takara (Dalian, China; Product n. 9108). NovoScript® Plus All-in-one 1st Strand cDNA Synthesis SuperMix was obtained from Novoprotein (Shanghai, China; Product n. E047). Hieff® qPCR SYBR Green Master Mix was obtained from Yeasen Biotechnology Co., Ltd (Shanghai, China; Product n. 11201ES08).

2.2. Nanoplastics preparation and characterization

NPs were characterized by use of transmission electron microscopy (TEM), dynamic light scattering (DLS), and fourier transform infrared spectroscopy (FTIR). Morphologies of NPs were characterized by use of TEM (JEM-2800, Japan) and we morphometrically assessed the images captured by TEM in the ImageJ software (NIH ImageJ, ver. 1.50 b) according to the studies of da Costa Araújo et al. (2020); de Oliveira et al. (2021); da Costa Araújo and Malafaia (2021); Guimarães et al. (2021a). The circularity was determined through the equation below.

$$Circularity(C) = 4\pi \frac{Area}{Permeter^2}$$

Hydrodynamic diameters and z-potentials of NPs were made by DLS performed by use of a Zetasizer Nano ZS90 (Malvern Instruments, Worcestershire, UK) which is equipped with Zetasizer software (version 7.12). Measures were conducted at 10 μg/mL NPs in ultrapure water and cell medium subjected to ultra-sonication (n = 3/group). The chemical composition of NPs was analyzed by a Bruker Tensor 27 FTIR spectrometer (Bruker, Karlsruhe, Germany).

2.3. Cell culture

A549 cells were grown in RPMI-1640 medium supplemented with 10% inactivated FBS, 100 U/mL penicillin and 100 μg/mL streptomycin. Cells were maintained in a humidified incubator at 37 °C and 5% CO_2. When confluent, cells were detached enzymatically with Trypsin-EDTA and sub-cultured into a new cell culture flask. The medium was replaced every 2 days. Logarithmically growing cells were used for experiments.

2.4. Cellular uptake of NPs

A549 cells were seeded in confocal dish and treated without or with 20 μg/mL green fluorescent NPs (n = 5/group). After 24 h, cells were washed three times with PBS buffer to eliminate residual medium and non-internalized NPs adhered to surfaces of cells. Cells were fixed at room temperature for 20 min with 4% paraformaldehyde to cross link proteins. Cell nuclei were stained with DAPI. Fluorescence images were obtained using a confocal laser scanning microscope (LSM880 with Airyscan, Zeiss, Germany).

2.5. Cytotoxicity tests

In order to evaluate effects of NPs alone on A549 cell viability, NPs at 10, 20, 100, 200, 500 or 1000 μg/mL were suspended in cell medium, and cell medium was used as a control. Before use, all NPs dispersions were ultrasonically treated to prevent aggregation. A549 cells were plated in 96-well culture plates at a cell density of 8×10^3 cells per well with 100 μL of cell medium and pre-incubated overnight. After 12 h, the culture medium was removed and 100 μL of prepared above test solutions were added (n = 5/group). Viability of A549 cells after 24 h of exposure were measured by using a CCK-8 assay based on procedures described by Shi et al. (2019b). CCK-8 kit utilizes water-soluble tetrazolium salt-SST-8 (WST-8), which is reduced by dehydrogenases of cells, to give soluble orange colored formazan. The amount of the formazan dye generated by dehydrogenase is directly proportional to the number of living cells. 10 μL of CCK-8 solution was added to each well and then cells were incubated for a further 4 h at 37 °C. The absorbance correlating to the number of living cells was measured at 450 nm with a microplate reader (Synergy H4, Bio-Tek, Vermont, USA). The cytotoxicity test was performed in triplicate.

Effects of co-exposure to combinations of NPs and DEHP or DBP on cellular viability were assessed. DEHP and DBP at concentration of 5 μg/mL in cell medium were prepared for test, the concentration of methanol in all test solutions were less than 0.01%. The used concentration of DEHP/DBP fall within the range of concentrations (0.1 μg/mL to 1.95 mg/mL) tested in different studies (Gao et al., 2019; Li et al., 2020a, 2020b; Lotfy et al., 2018; Molino et al., 2019; Peropadre et al., 2015, 2013), and the interaction between relatively high level of DEHP/DBP with NPs is possible and of great significance as it's reported that partitioning of organic compounds from seawater to polymer plastics is about six orders of magnitude greater in plastics than in seawater (Mato et al., 2001; Wright et al., 2013). The concentrations of 20 or 200 μg NPs/mL for NPs were used in the co-exposure as they fall within the range of concentrations (0.05 μg/mL to 500 μg/mL) tested in different in vitro studies in cells (Cortés et al., 2020; Prietl et al., 2014; Schirinzi et al., 2017; Wang et al., 2020b; Wu et al., 2019; Xu et al., 2019) and the range of concentrations (0.8 μg/L to 2 g/L, or 1000–1800000 p/L and 0.0003% of plastics in water) in vivo studies (Estrela et al., 2021; Kögel et al., 2020), and the relatively high level of NPs could simulate highly pessimistic pollution scenarios identified at points close to pollution sources. In total, nine treatments were used including: 1) only complete medium (control); 2) 20 μg NPs/mL (NPL); 3) 200 μg NPs/mL (NPG); 4) 5 μg DBP/mL (DBP); 5) 20 μg NPs/mL combined with 5 μg DBP/mL (NPL+DBP); 6) 200 μg NPs/mL combined with 5 μg DBP/mL (NPG+DBP); 7) 5 μg DEHP/mL (DEHP); 8) 20 μg NPs/mL combined with 5 μg DEHP/mL (NPL+DEHP); 9) 200 μg NPs mL combined with 5 μg DEHP/mL (NPG+DEHP). The CCK-8 assay was performed in the same manner described above (n = 5/group) and test was performed in triplicate.

2.6. Size distribution

To characterize the distribution of sizes of NPs in the presence of DBP and DEHP, after 24 h, DLS was performed with a Zeta Sizer instrument (Nano ZS90, Malvern Instruments, Worcestershire, UK). Measurements were conducted at 37 °C, without sonication, using 20 μg NPs/mL or 200 μg NPs/mL in the presence or absence of DBP or DEHP for 24 h incubation in the test media (n = 3/group). Determinations were performed in triplicate.

2.7. Quantification of PAEs

To monitor concentrations of DBP and DEHP (with an initial concentration at 5 μg/mL in the presence of 20 or 200 μg NPs/mL), cell medium and cells were collected after exposure for 24 h (n = 3/group). Concentrations of DBP and DEHP were determined according to previously published methods (Li et al., 2020a, 2020b) with modifications. Briefly, after being filtered through 0.02 μm hydrophilic polyvinylidene fluoride membranes, cell medium mixed with D_4-DBP or D_4-DEHP isotope internal standards were subjected to liquid phase extraction (LPE) with normal hexane. Organic phases were determined by gas chromatography-mass spectrometry (GC-MS) (7890B-5977B, Agilent, USA) with an electron ionization (EI) source on a 5% phenyl methyl polysiloxane capillary column (length: 30 m; inner diameter: 0.250 mm; thickness: 0.25 μm). Cells were ground, vortexed, and sonicated in normal hexane. The DBP and DEHP were extracted using LPE and the organic phases were collected for GC-MS analysis. The coefficient of determination for a standard curve, which included six concentrations: 0, 10, 20, 80, 200 or 400 ng/mL was greater than 0.99. Temperature increasing program at working conditions of the GC-MS is as follows: 80 °C isotherm for 3 min, 20 °C/min till 220 °C and isotherm for 1 min, then 50 °C/min till 300 °C and isotherm for 10 min. The carrier gas was high purity (99.999%) helium and the mass spectrometer was operated in selected ion monitoring mode. In addition, the quantification of NPs was also performed according to previous study (Estrela et al., 2021) with some modifications, and the detailed analysis procedures are provided in the Text S1.

2.8. Estimation of production of ROS

Intracellular ROS were measured by use of a ROS assay kit, containing a sensitive fluorescent probe 2,7-dichlorofluorescin diacetate (DCFH-DA) which has no fluorescence and can freely cross the cell membrane. However, after entering the cell, it can be hydrolyzed by intracellular esterase to produce 2,7-dichlorofluorescin (DCFH) and then intracellular ROS can oxidize non-fluorescent DCFH to produce fluorescent 2, 7-dichlorofluorescein (DCF). By detecting the fluorescence of DCF (λ_{ex} = 488 nm and λ_{em} = 525 nm), we can know the level of ROS in the cell. Herein, A549 cells cultured in tissue culture plates were exposed to different treatments for 24 h (n = 5/group). Then, cells were washed three times with PBS and incubated with serum-free cell medium containing 10 μM DCFH-DA for 20 min at 37 °C in dark. Subsequently, cells were rinsed three times with PBS and harvested in PBS. Fluorescent intensities were measured on a microplate reader (Synergy H4, Bio-Tek, Vermont, USA). The experiment was repeated three times.

2.9. Measurement of SOD, CAT, GSH-Px and MDA

Intracellular SOD, CAT, GSH-Px and MDA activities were determined by use of a total SOD assay kit, total CAT assay kit total, GSH-Px assay kit and MDA assay kit, respectively. After 24 h of treatment, the cells in each treatment group were washed with cold PBS, and then lysed in cell lysis buffer and centrifuged at 12,000 g at 4 ℃ for 10 min. Supernatants were used to detect the intracellular enzyme activities of SOD, CAT, GSH-Px and MDA content, according to the manufacturer's instructions of each assay kit (n = 5/group) and performed for 3 times. Thereinto, the total SOD assay kit was based on WST-8 method. According to the manufacturer's instruction, 20 μL of each sample was pipetted into microplate wells and then filled with 160 μL WST-8 working solution and 20 μL of the reaction start-up working solution. After incubation at 37 ℃ for 30 min, the absorbance at 450 nm was measured on a

microplate reader (Synergy H4, Bio-Tek, Vermont, USA) to indicate the activity of SOD. The total CAT assay kit was based on a color reaction that the hydrogen peroxide can oxidize the chromogenic substrate under the catalysis of peroxidase to produce a red product (N-(4-antipyryl)−3-chloro-5-sulfonate-p-benzoquinonemonoimine) with a largest absorption wavelength at 520 nm. According to the manufacturer's instruction, we pipetted 40 μL of each sample and 10 μL hydrogen peroxide solution of 250 mM into microplate wells to react at 25 °C for 5 min and then the chromogenic working solution was added to react at 25 ℃ for 20 min. The absorbance at 520 nm was measured on a microplate reader (Synergy H4, Bio-Tek, Vermont, USA) to indicate the activity of CAT. The total GSH-Px assay kit is based on the nicotinamide adenine dinucleotide phosphate (NADPH) method that GSH-Px can catalyze glutathione (GSH) to produce glutathione disulfide (GSSG), while glutathione reductase can use NADPH to catalyze GSSG to produce GSH. 50 μL of each sample was pipetted into microplate wells and then added with 40 μL GSH-Px detection working solution (mixture of NADPH, GSH and glutathione reductase) to incubate at room temperature for 15 min 10 μL of 30 mM peroxide solution was added into each well and the absorbance at 340 nm was measured on a microplate reader (Synergy H4, Bio-Tek, Vermont, USA) to indicate the activity of GSH-Px. The MDA assay kit is based on a color reaction that MDA can react with thiobarbituric acid (TBA) to produce a red product. 100 μL of each sample was pipetted into eppendorf tubes and then 200 of MDA detection working solution (mixture of TBA and antioxidant) was added. After mixing, each mixture was treated with boiling water bath for 15 min and centrifuge at 1000 g at room temperature for 10 min after cooling to room temperature. The absorbance at 532 nm was measured on a microplate reader (Synergy H4, Bio-Tek, Vermont, USA) to indicate the content of MDA. Total protein was measured with a BCA protein assay kit. The results were expressed as U/mg protein for SOD, U/mg protein for CAT, U/mg protein for GSH-Px and nmol/mg protein for MDA.

2.10. mRNA extracts and quantitative real-time PCR (qPCR) analysis

Transcription of mRNAs of genes, interleukin 1β (IL-1β), interleukin 8 (IL-6), interleukin 8 (IL-8) and tumor necrosis factor (TNF-α), associated with pro-inflammatory cytokines, were analyzed using qPCR. Herein, A549 cells were plated separately in 6-well plates and exposed to different treatments for 24 h (n = 3/group). Then, total RNA was extracted with RNAiso Plus reagent according to manufacturer's instructions. Total RNA was quantified and qualified with a microspectrophotometer (Nano-100, All Sheng, China) by measuring the absorbance at 260 and 280 nm.

Synthesis of cDNAs and qPCR were performed according to the recommended manufacturer's protocols of the NovoScript® Plus All-in-one 1st Strand cDNA Synthesis SuperMix and Hieff® qPCR SYBR Green Master Mix. The sequence of primers used was shown in Table S2. Experiments were repeated at least three times. Relative quantification of expressions of target genes was measured using GAPDH mRNA as an internal control. The comparative $2^{-\Delta\Delta Ct}$ method was used to evaluate the relative expression of mRNA. This experiment was performed for 3 times.

2.11. Statistical analysis

GraphPad Prism Software Version 8.0 (San Diego, CA, USA) was used for statistical analysis. Data were checked for deviations from normality of variance and homogeneity of variance before analysis. Normality of data was assessed by use of the Shapiro-Wilks test, and homogeneity of variance was assessed by use of Bartlette's test. If necessary, data was log10-transformed to better approximate normality and homogeneity of variance. Single comparisons were carried out using a paired Student's *t*-test. Multiple comparisons were performed using a one-way ANOVA and Tukey's post-hoc analysis. Levels of significance were set at values of Type I error (*p*) less than 0.05, 0.01 or 0.001. Data are expressed as the mean ±SEM.

3. Results and discussion

A control exposure to methanol was conducted to assess toxicity of the solvent to A549 cells. There was no significant difference in viabilities of cells, generation of ROS, performance of antioxidant systems or inflammatory response between the solvent control and negative control groups ($P > 0.05$) (Fig. S1), which indicates the solvent, methanol had no significant effects on any of the parameters measured in A549 cells.

3.1. Characterization of NPs

Characteristics of NPs were slightly affected by the culture medium. Based on TEM images (Fig. 1 A and B) and the determined circularity (0.970 ± 0.006), NPs displayed a uniformly spherical shape. DLS analysis revealed that the hydrodynamic diameter of NPs in ultrapure water was 104.77 ± 1.47 nm, but slightly larger in cell medium (117.23 ± 1.96 nm) (Fig. 1 C), which was consistent with results of previous study of Ruenraroengsak and Tetley (2015) that they measured that the hydrodynamic diameter of polystyrene NPs in cell medium (123.80 ± 0.18 nm) was slightly larger than that in ultrapure water (101.60 ± 1.08 nm) and might be due to adsorption of proteins and other components of the medium onto the NPs (Ruenraroengsak and Tetley, 2015; Xia et al., 2008). These findings were also indicated by the polydispersity index (PDI) (Table S3). The zeta potential of NPs in ultrapure water (−16.30 ± 1.07 mV) was more negative than that in cell medium (−4.77 ± 1.02 mV), which is corresponding to the previous researches (Chiu et al., 2015; Ruenraroengsak et al., 2012). In addition, the comparison of the FTIR spectra of the studied NPs samples (Fig. S2) with typical infrared absorption peaks of the polystyrene material (Ding et al., 2020; Liu et al., 2020, 2019b; Lu et al., 2018b; Mao et al., 2020) confirmed that the assessed particles are polystyrene NPs.

3.2. Cytotoxicity

A549 cells, which are a good model for human alveolar type II pulmonary epithelium, have been widely employed for determining toxicology, pharmacology, injury to and metabolic processing of lung tissue in vitro (Huang et al., 2019; Shi et al., 2019a; Xu et al., 2019). During this study, NPs with mean diameter of 117.23 ± 1.96 nm passed into A549 cells and were accumulated in the cytoplasm (Fig. 2 A and B). In the cells exposed to green fluorescent NPs (Fig. 2 B), green fluorescence was present, which suggested the presence of NPs. This result was consistent with previous results (Deville et al., 2015; Xu et al., 2019) that demonstrated accumulation of NPs in A549 cells as Xu et al. (2019) have detected the internalization of the polystyrene NPs of 25 and 75 nm and Deville et al. (2015) have observed the uptake of polystyrene NPs of 116 ± 1 nm in A549 cells. The major uptake pathway of plastic particles has been reported to be endocytosis (Lehner et al., 2019). The widely distributed NPs in A549 cells might subsequently result in some effects on performance, which suggests potential damage to lungs. In order to assess effects of NPs on viability of A549 cells, greater concentrations of NPs were added to A549 cells and incubated for 24 h, and cell viability was determined by use of the CCK-8 assay. NPs had no significant effects on viability of A549 cells at concentrations less than 100 μg/mL, but exhibited cytotoxicity at concentrations greater than 200 μg NPs/mL (Fig. 2 C). Therefore, 20 and 200 μg NPs/mL, herein referred to as a lesser concentration (NPL) and greater concentration (NPG) of NPs, respectively, were selected for following study to measure effect of NPs on toxic potencies of DEHP and DBP to A549 cells. Cytotoxicities of co-exposure to DEHP or DBP in presence or absence of NPs were investigated. Exposure to either DEHP-only or DBP-only caused significant cytotoxicity at 5 μg/mL (Fig. 2 D), results which are consistent with other studies (Lotfy et al., 2018; Peropadre et al., 2013; Yu et al., 2009). Compared with the DBP-only or DEHP-only treatments,

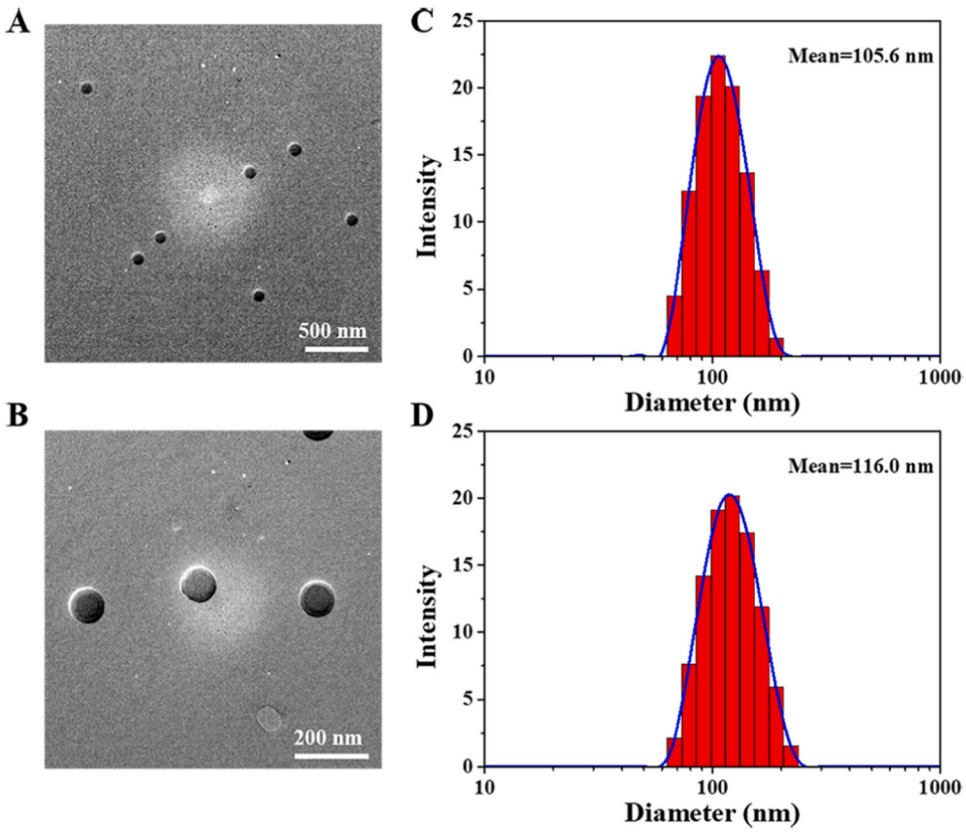

Fig. 1. Characterization of NPs. (A) Low-magnitude transmission electron microscopy image of NPs; (B) High-magnitude transmission electron microscopy image of NPs; (C) The representative size distribution of NPs in ultrapure water; (D) The representative size distribution of NPs in ultrapure cell medium.

cytotoxicity to A549 cells was less for exposure to both NPL+DBP and NPL+DEHP, while greater for both NPG+DBP and NPG+DEHP, which indicates that cytotoxicity due to co-exposure with NPs and DBP or DEHP varied as a function of concentration of NPs. Effects of NPs at the lesser concentration on cytotoxicity of DEHP were greater than for DBP and the combined cytotoxicity of NPs at the greater concentration and DBP or DEHP were similar to cytotoxicity caused by of NPG-only. Cytotoxicity of combined exposure to NPs and DBP or DEHP on A549 were still greater than NPs-only treatments, which indicates co-exposure is still hazardous.

3.3. *Effects of NPs on bioavailability of DEHP and DBP*

Partitioning of organic compounds from seawater to polymer plastics is about six orders of magnitude greater in plastics than in seawater (Mato et al., 2001; Wright et al., 2013). Hydrophobicity and lipophilicity of these organic compounds and surface-volume ratio of the plastic particles might be responsible for sorption capacity of plastic particles for contaminants (Liu et al., 2016; Rodrigues et al., 2019). Interactions between microplastics and PAEs have been suggested to have greater sorption capacity of tested PAEs on PS plastic particles than PE or PVC plastic particles (Liu et al., 2019a). Partitioning was the main mechanism of sorption and the hydrophobic interaction governed the partition mechanism (Liu et al., 2019a).

Because sorption of contaminants by plastic particles might be one of the reasons for observed differences in toxicity and bioavailability (Li et al., 2020a; Liu et al., 2019a; Sørensen et al., 2020; Wang et al., 2019), DLS were measured to investigate such interactions of NPs incubated with or without PAEs after 24 h (Fig. S3). The results indicated that in the absence of PAEs, NPs exhibited relatively little aggregation because average diameters of NPL and NPG were 120.73 ± 1.48 nm and 122.33 ± 1.11 nm, respectively. The mean diameter in NPL+DBP was 135.63 ± 2.21, while that in NPG+DBP was 142.13 ± 0.68 nm. Particle diameters were 150.87 ± 2.08 and 162.37 ± 0.24 nm, respectively in NPL+DEHP and NPG+DEHP. Moreover, the quantification of NPs has been shown in Table S4. To further investigate sorption, quantitation of DEHP and DBP after co-exposure was investigated (Table 1). In the control group, free concentrations (C_{free}) of PAEs in cell medium and PAEs concentrations in cells were not detected. And in the NPL and NPG groups, the C_{free} of PAEs in cell medium and PAEs concentrations in cells were both small, which indicated that the amount of PAEs in NPs was negligible. The C_{free} of DBP in cell medium of the DBP-only exposure or combined exposures NPL+DBP and NPG+DBP were 3.83 ± 0.09, 3.60 ± 0.05 and 3.27 ± 0.03 μg/mL, respectively, which indicated significantly lesser C_{free} of DBP in NPL+DBP ($p < 0.05$) and NPG+DBP group ($p < 0.001$) compared to DBP-only, whereas C_{free} of DEHP exhibited more significant reductions in NPL+DEHP and NPG+DEHP with p-values both less than 0.001, compared to exposure to DEHP-only. Concentrations of DBP and DEHP in cells, were all less than for the combined exposures compared to their respective single exposures.

Numerous studies have shown that plastic particles can sorb organic compounds and influence their free concentrations in solution (Li et al., 2020a; Sørensen et al., 2020; Trevisan et al., 2019). PAHs, which are fairly hydrophobic organic compounds, have been shown to sorb to surfaces of the MPs and NPs as shown in combined exposure studies of PAHs with polystyrene MPs of 10 μm (Sørensen et al., 2020) and polystyrene NPs of 44 nm (Trevisan et al., 2019), that resulted in lesser freely dissolved concentrations and toxicity (Sørensen et al., 2020; Trevisan et al., 2019). Concentrations of freely dissolved DBP was less in the presence of polystyrene NPs of 100 nm at 1 and 20 μg/mL (Li et al., 2020a, 2020b). In addition, the authors pointed out that it was adsorption to plastic particles that led to decreased bioavailability of DBP, resulting in decreased toxicity of DBP. Alternatively, adsorption of arsenic (As) to polystyrene MPs in cell medium suggested that both

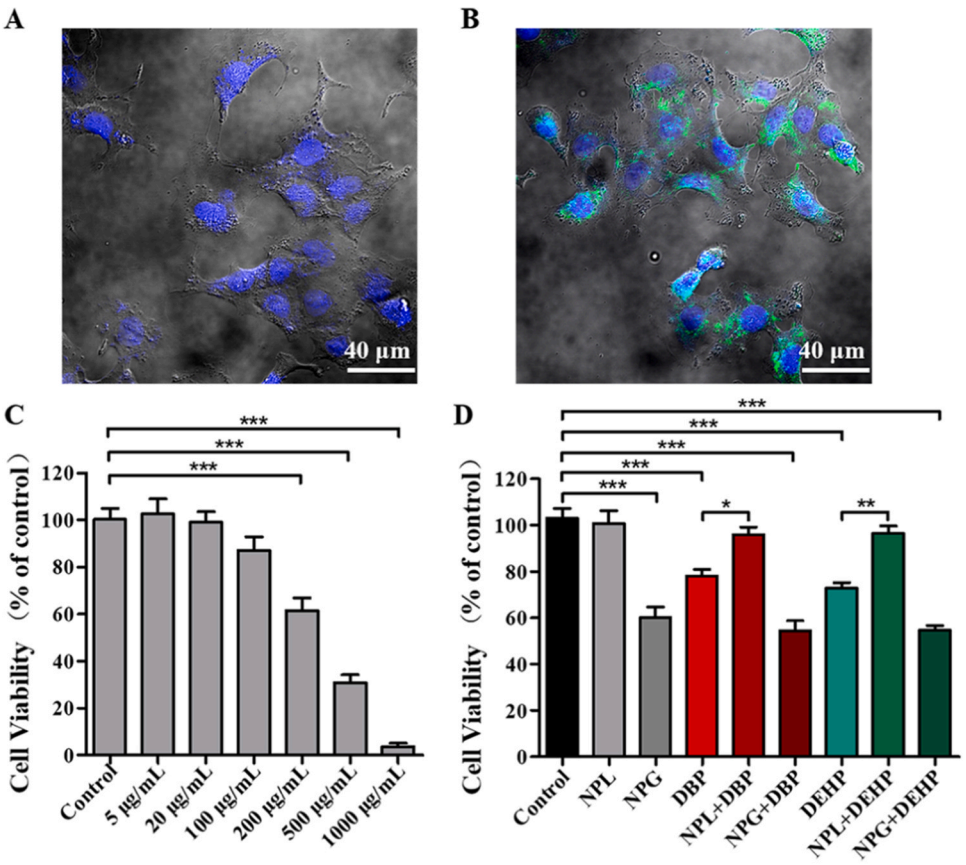

Fig. 2. Accumulation of NPs by A549 cells and cell viability of A549 cells with different treatments. (A) Image of confocal microscopy of A549 cells treated without NPs for 24 h; (B) The image of confocal microscopy of A549 cells treated with green fluorescent polystyrene NPs of 20 μg/mL at 24 h; (C) Effects of NPs in gradient concentration on viability of A549 cells; $F_{(6,\ 27)} = 68.33$, $p < 0.0001$; (D) The effects of the co-exposure of NPs and phthalate esters on viability of A549 cells; $F_{(8,\ 35)} = 28.94$, $p < 0.0001$. $^{*}p < 0.05$, $^{**}p < 0.01$, $^{***}p < 0.001$. control: control group; NPL: group exposed to 20 μg/mL polystyrene nanoplastics; NPG: group exposed to 200 μg/mL polystyrene nanoplastics; DBP: group exposed to 5 μg/mL dibutyl phthalate; NPL+DBP: group co-exposed to 20 μg/mL polystyrene nanoplastics and 5 μg/mL dibutyl phthalate; NPH+DBP: group co-exposed to 200 μg/mL polystyrene nanoplastics and 5 μg/mL dibutyl phthalate; DEHP: group exposed to 5 μg/mL di-(2-ethylhexyl) phthalate; NPL+DEHP: group co-exposed to 20 μg/mL polystyrene nanoplastics and 5 μg/mL di-(2-ethylhexyl) phthalate; NPH+DEHP: group co-exposed to 200 μg/mL polystyrene nanoplastics and 5 μg/mL di-(2-ethylhexyl) phthalate.

Table 1
Free phase concentrations (C_{free}) of phthalate esters in cell culture medium and phthalate esters concentrations in cells in different treatment groups.

	Nominal concentrations of NPs (μg/mL)	Nominal concentration of PAEs (μg/mL)	C_{free} of PAEs in cell culture medium (μg/mL)	PAEs concentrations in cells (ng/10^3 cells)
Control	0	0	n.d.	n.d.
NPL	20	0	0.0051 ± 0.0007	0.0021 ± 0.0002
NPG	200	0	0.0062 ± 0.0005	0.0031 ± 0.0003
DBP	0	5	3.83 ± 0.09	1.91 ± 0.05
NPL+DBP	20	5	3.60 ± 0.05*	1.74 ± 0.05*
NPG+DBP	200	5	3.27 ± 0.03***	1.62 ± 0.06***
DEHP	0	5	3.73 ± 0.08	1.85 ± 0.06
NPL+DEHP	20	5	3.30 ± 0.05###	1.65 ± 0.05##
NPG+DEHP	200	5	2.85 ± 0.09###	1.51 ± 0.01###

n.d.: not detected. Numerical data represent the mean ±standard deviation. * Indicates significant difference between DBP-only exposure and combined of DBP and NPs groups (*$p < 0.05$, ***$p < 0.001$). # Indicates significant difference between DEHP-only exposure and combined exposure of DEHP and NPs (##$p < 0.01$, ###$p < 0.001$). PAEs: phthalate esters. control: control group; NPL: group exposed to 20 μg/mL polystyrene nanoplastics; NPG: group exposed to 200 μg/mL polystyrene nanoplastics; DBP: group exposed to 5 μg/mL dibutyl phthalate; NPL+DBP: group co-exposed to 20 μg/mL polystyrene nanoplastics and 5 μg/mL dibutyl phthalate; NPH+DBP: group co-exposed to 200 μg/mL polystyrene nanoplastics and 5 μg/mL dibutyl phthalate; DEHP: group exposed to 5 μg/mL di-(2-ethylhexyl) phthalate; NPL+DEHP: group co-exposed to 20 μg/mL polystyrene nanoplastics and 5 μg/mL di-(2-ethylhexyl) phthalate; NPH+DEHP: group co-exposed to 200 μg/mL polystyrene nanoplastics and 5 μg/mL di-(2-ethylhexyl) phthalate.

0.1 μm (20 μg/mL) and 5 μm (80 μg/mL) polystyrene MPs weakly adsorbed As (Wu et al., 2019). Intracellular concentrations of As in Caco-2 cells were less in the presence of 0.1 μm PS MPs, while those in the presence of 5 μm PS MPs were not (Wu et al., 2019). These divergent results might due to properties of both the chemicals and plastic particles (Schönlau et al., 2019). In present study, the combination of NPs and PAEs reduced the concentration of free PAEs in cell medium and cell burden of PAEs, which confirmed that the large surface to volume ratio of the plastic particles and the hydrophobic nature of NPs and PAEs drove the sorption of free PAEs to NPs and decreased the uptake. DEHP was much more hydrophobic than DBP with greater logK_{ow} and lesser solubility (Table S2), which resulted in the greater sorption capacity to NPs and lesser concentration of free DEHP than DBP, which resulted in greater reduction in cytotoxicity in the presence of small concentrations of NPs. In addition to strong sorption, lesser bioavailability of chemical contaminants might be also associated with the little desorption (Tourinho et al., 2019). There was enhanced desorption of persistent organic pollutants from plastic particles under simulated physiological gut fluid conditions (pH 4 at 38 ℃) (Bakir et al., 2014). Results of other studies have emphasized that the properties of the solution can affect desorption of chemicals on plastic particles (Bakir et al., 2014; Liu et al., 2019a; Tourinho et al., 2019). Therefore, we postulate that desorption of chemicals from plastics under intracellular conditions might be different from that observed in simulated physiological gut fluid or pure water.

The relatively great cytotoxicity observed where concentrations of NPs and PAEs were greatest, might be due to the predominant role in combined cytotoxicity of NPs when present at greater concentrations. This conclusion is consistent with results of previous study that the polystyrene NPs of 100 nm dominated the toxicity when the concentration of polystyrene NPs was high enough (1–75 μg/mL) during the co-exposure of polystyrene NPs and polychlorinated biphenyls to *Daphnia magna* (Lin et al., 2019). Furthermore, greater toxicity to caco-2 cells was observed at the exposure to a relatively great concentration (120 μg/mL) of polystyrene NPs of 300 and 500 nm combined with bisphenol A (Wang et al., 2020b).

3.4. Mechanism of toxicity to cells of co-exposure to PAE and NPs

It has been confirmed that reactive oxygen species (ROS) (e.g., superoxide, singlet oxygen, and H_2O_2), types of free radicals, can be generated by exogenous agents including environmental contaminants. Accordingly, PAEs have been verified to induce the release of reactive oxygen species (ROS) sequentially causing oxidative stress in in vitro and animal studies (Kasahara et al., 2002; Zhao et al., 2012). Likewise, plastic particles can also trigger ROS (Meindl et al., 2015; Poma et al., 2019; Schirinzi et al., 2017; Wang et al., 2020b), For example, Wang et al. (2020b) have detected that the polystyrene NPs (300 and 500 nm) and MPs (1, 3 and 6 μm) at 120 μg/mL all increased the production of ROS. Oxidative stress induced by ROS is considered to be the probable mechanism of toxicity induced by MPs and NPs (Prata et al., 2020). In fact, there is a balance between generation of pro-oxidants and their neutralization by antioxidants (Ahamed et al., 2019). Formation of larger amounts of ROS can overcome the cellular antioxidant enzyme capacity, such as SOD, CAT and GSH-Px, leading to considerable oxidative stress. Hence, the assessment of intracellular ROS, evaluation of antioxidant enzyme activity was conducted. Besides, conditions that lead to tissue damage might be facilitated by ROS, with inflammation being the initial reaction to tissue damage (Dong et al., 2020). Oxidative stress and inflammation are closely associated with pathophysiological processes, even one of which can be easily motivated by another (Lu et al., 2018a; Tousoulis et al., 2008). Here, the inflammatory response was also measured. Collectively, these results confirmed that oxidative stress and inflammatory response accounted for the underlying cytotoxic mechanisms of combined exposure to PAE and NPs.

3.4.1. Oxidative stress

The DCFH-DA probe was applied to determine the intracellular ROS in A549 cells in this study (Fig. 3). Compared to control group, the NPG group was detected significantly enhanced amounts of ROS, which was consistent with previous results that generation of ROS was significantly greater in human lung cells after exposure to polystyrene NPs as Lim et al. (2019) observed the increased ROS level in human bronchus epithelial BEAS-2B cells treated with polystyrene NPs of 60 nm at 10 and 50 μg/mL. Amounts of ROS in A549 cells in DBP-only group and DEHP-only group were significantly greater than those in the control group, a result that was similar to those of the previous study (Kim et al., 2019). Addition of NPs at the lesser concentration resulted in less ROS co-exposed with PAEs. There was less ROS produced in NPL+DBP group ($p < 0.05$) and NPL+DEHP group ($p < 0.01$) compared with cells exposed to DBP-only or DEHP-only, respectively. However, greater accumulation of ROS was observed when exposed to NPG+DBP or NPG+DEHP compared with DBP-only or DEHP-only, respectively. Contents of ROS in cells exposed to NPG+DBP or NPG+DEHP were greater reaching concentrations 1.72- and 1.71-fold greater than that of the controls, respectively, but were not different from cells exposed to NPG. Concentrations of ROS for DBP and DEHP were less in the presence of the lesser concentration of NPs. This effect due to the presence of the small concentration of NPs was greater for DEHP than for DBP. However, the amount of ROS in cells exposed to DBP or DEHP were both greater in the presence of the greater concentration of NPs. In fact, they

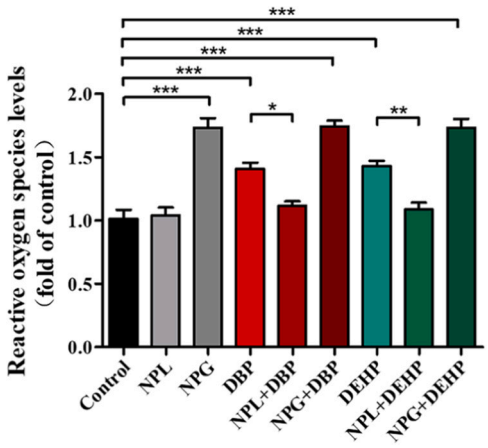

Fig. 3. Effects on intracellular generation of reactive oxygen species in A549 cells after 24 h exposure to of co-exposure to NPs and phthalate esters; $F_{(8, 35)} = 28.98$, $p < 0.0001$. $^{*}p < 0.05$, $^{**}p < 0.01$, $^{***}p < 0.001$. control: control group; NPL: group exposed to 20 μg/mL polystyrene nanoplastics; NPG: group exposed to 200 μg/mL polystyrene nanoplastics; DBP: group exposed to 5 μg/mL dibutyl phthalate; NPL+DBP: group co-exposed to 20 μg/mL polystyrene nanoplastics and 5 μg/mL dibutyl phthalate; NPH+DBP: group co-exposed to 200 μg/mL polystyrene nanoplastics and 5 μg/mL dibutyl phthalate; DEHP: group exposed to 5 μg/mL di-(2-ethylhexyl) phthalate; NPL+DEHP: group co-exposed to 20 μg/mL polystyrene nanoplastics and 5 μg/mL di-(2-ethylhexyl) phthalate; NPH+DEHP: group co-exposed to 200 μg/mL polystyrene nanoplastics and 5 μg/mL di-(2-ethylhexyl) phthalate.

were approximately equivalent to those of cells exposed to the greater concentration of NPs alone. All these results might be related to intracellular accumulation and bioavailability. In addition, excessive production of ROS might lead to oxidative stress, which could subsequently cause the pathological processes of many diseases including respiratory diseases. It has been suggested that ROS can stimulate oxidative damage of macromolecules, such as nucleic acids, lipids and proteins inducing lung cell death, loss of alveolar units and development of chronic obstructive pulmonary disease (COPD) (Langen et al., 2003; Zhou et al., 2019; Zhu et al., 2019). Therefore, the adverse effects of co-exposure of PAE and NPs resulted from production of ROS on lung are worthy of attention.

To elucidate the role of oxidative stress in combined cytotoxicity, SOD, CAT, GSH-Px activities and concentrations of the product of lipid peroxidation, malondialdehyde (MDA) in A549 cells were quantified (Fig. 4). It had been reported that imbalances in oxidants and antioxidants resulting in oxidative stress might have a potential role in pathogenesis of lung diseases (Zhu et al., 2019; Zuo et al., 2014). The antioxidant enzymes, SOD, CAT and GSH-Px play crucial roles in resistance to oxidative damage (Wang et al., 2020a). Of these, SOD, which can turn dismutation of superoxide into molecular oxygen and hydrogen peroxide reducing the occurrence of lipid peroxidation is usually considered to be the primary enzyme to treat ROS (Gao et al., 2019; Pandey et al., 2003; Wang et al., 2020a). CAT is able to remove ROS and provides resistance to oxidative damage by transforming H_2O_2 to water and oxygen (Chen et al., 2018; Rengel et al., 2005; Wang et al., 2020a). GSH-Px, which is responsible for inactivation of lipid peroxidase, can remove superoxide anion radical (Anand et al., 2012; Wang et al., 2020a). Activities of SOD, CAT and GSH-Px were less in exposures other than the control. There were significant differences between the controls and exposures to NPG-only, DBP-only, NPG+DBP, DEHP-only and NPG+DEHP. Moreover, exposure to NPL+DBP exhibited significant increments in activities of SOD ($p < 0.05$), CAT ($p < 0.01$) and GSH-Px ($p < 0.05$), while exposure to NPL+DEHP also resulted in greater increments in activities of SOD ($p < 0.001$), CAT ($p < 0.001$) and GSH-Px ($p < 0.01$) compared to exposures to DBP-only and DEHP-only. Activities of SOD, CAT and GSH-Px were less in cells exposed to either

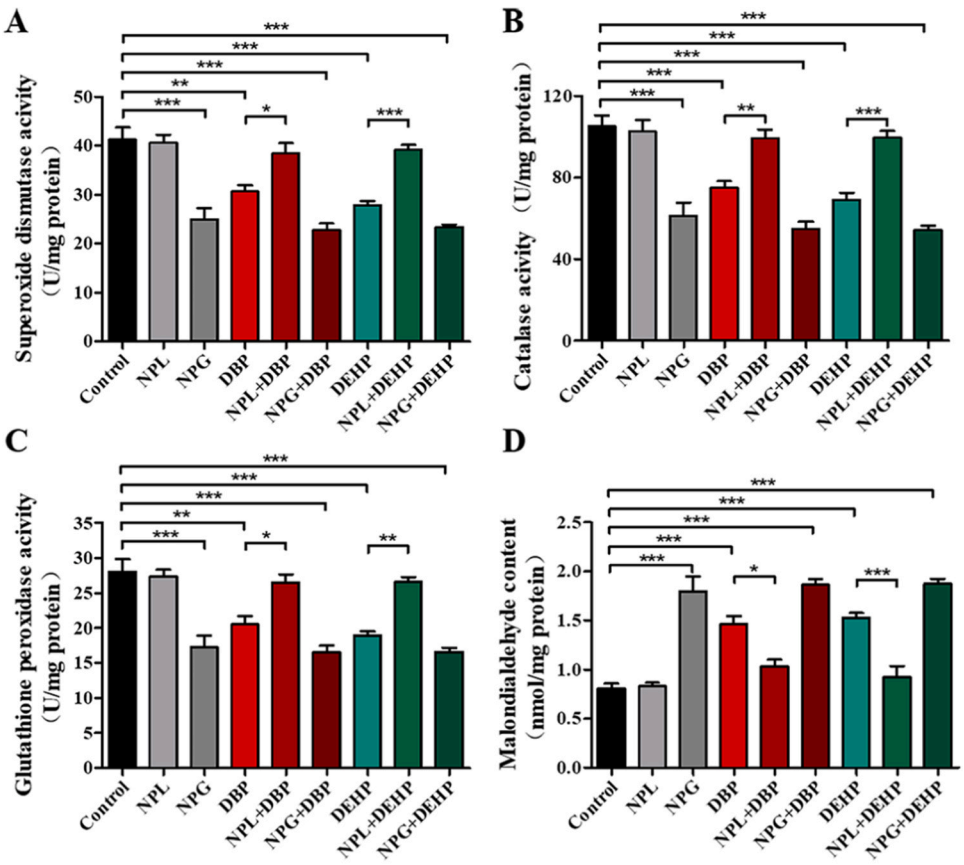

Fig. 4. Effects on the antioxidant system in A549 cells after 24 h co-exposure to NPs and phthalate esters. (A) Effects on the activity of superoxide dismutase; $F_{(8,\ 35)} = 21.77$, $p < 0.0001$; (B) Effects on the activity of catalase; $F_{(8,\ 35)} = 23.82$, $p < 0.0001$; (C) Effects on the activity of glutathione peroxidase; $F_{(8,\ 35)} = 18.71$, $p < 0.0001$; (D) Effects on concentrations of malondialdehyde; $F_{(8,\ 35)} = 31.48$, $p < 0.0001$. $^{*}p < 0.05$, $^{**}p < 0.01$, $^{***}p < 0.001$. control: control group; NPL: group exposed to 20 μg/mL polystyrene nanoplastics; NPG: group exposed to 200 μg/mL polystyrene nanoplastics; DBP: group exposed to 5 μg/mL dibutyl phthalate; NPL+DBP: group co-exposed to 20 μg/mL polystyrene nanoplastics and 5 μg/mL dibutyl phthalate; NPH+DBP: group co-exposed to 200 μg/mL polystyrene nanoplastics and 5 μg/mL dibutyl phthalate; DEHP: group exposed to 5 μg/mL di-(2-ethylhexyl) phthalate; NPL+DEHP: group co-exposed to 20 μg/mL polystyrene nanoplastics and 5 μg/mL di-(2-ethylhexyl) phthalate; NPH+DEHP: group co-exposed to 200 μg/mL polystyrene nanoplastics and 5 μg/mL di-(2-ethylhexyl) phthalate.

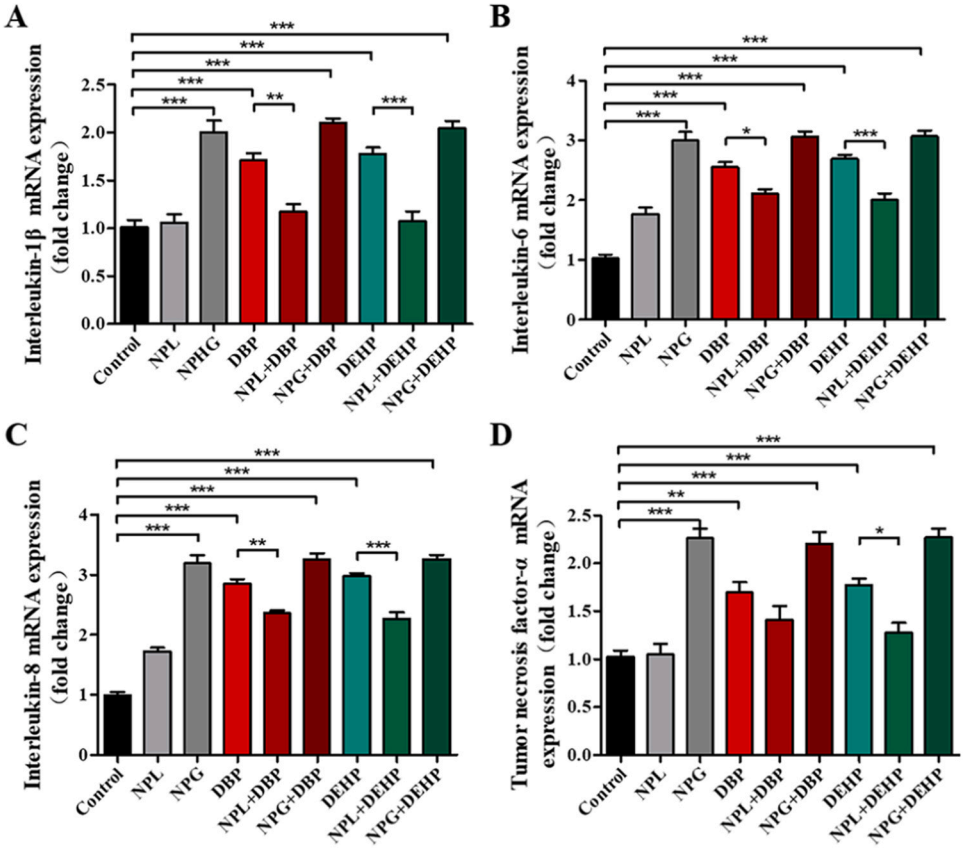

Fig. 5. Inflammatory response of A549 cells co-exposed for 24 h to NPs and PAEs. (A) Expression of mRNA for interleukin-1β; $F_{(8,\ 35)} = 31.71$, $p < 0.0001$; (B) expression of mRNA for interleukin-6; $F_{(8,\ 35)} = 54.36$, $p < 0.0001$; (C) Expression of mRNA for interleukin-8; $F_{(8,\ 35)} = 84.03$, $p < 0.0001$; (D) Expression of mRNA for tumor necrosis factor-α; $F_{(8,\ 35)} = 23.55$, $p < 0.0001$. $^{*}p < 0.05$, $^{**}p < 0.01$, $^{***}p < 0.001$. control: control group; NPL: group exposed to 20 μg/mL polystyrene nanoplastics; NPG: group exposed to 200 μg/mL polystyrene nanoplastics; DBP: group exposed to 5 μg/mL dibutyl phthalate; NPL+DBP: group co-exposed to 20 μg/mL polystyrene nanoplastics and 5 μg/mL dibutyl phthalate; NPH+DBP: group co-exposed to 200 μg/mL polystyrene nanoplastics and 5 μg/mL dibutyl phthalate; DEHP: group exposed to 5 μg/mL di-(2-ethylhexyl) phthalate; NPL+DEHP: group co-exposed to 20 μg/mL polystyrene nanoplastics and 5 μg/mL di-(2-ethylhexyl) phthalate; NPH+DEHP: group co-exposed to 200 μg/mL polystyrene nanoplastics and 5 μg/mL di-(2-ethylhexyl) phthalate.

NPG+DBP or NPG+DEHP and their activities were similar to those in cells exposed to NPG-only. MDA is the product of peroxidation of lipids (Klaunig et al., 2011), revealing oxidative stress and was proportional to severity of damage to cells (Wang et al., 2020a; Zhang et al., 2019a, 2019b). Results indicated that concentrations of MDA were significantly ($p < 0.05$) less in cells exposed to NPL+DBP with an even more significant ($p < 0.001$) reduction in cells exposed to NPL+DEHP. Alternatively, concentrations of MDA were greater than control cells exposed to either NPG+DBP or NPG+DEHP, compared to DBP-only and DEHP-only, respectively. Oxidative stress has been regarded as a crucial molecular mechanism of adverse effects induced by plastic particles (Prata et al., 2020). Results of this study demonstrated that NPs can cause oxidative stress by exceeding cellular antioxidant enzyme capacity. Responses to oxidative stress were less in cells exposed to a combination of PAEs and small concentration of NPs and enhanced in combination of PAEs and greater concentration of NPs.

3.4.2. *Inflammatory response*

Pro-inflammatory cytokines, such as IL-1β, IL-6, IL-8 and TNF-α, serve to stimulate the immune system, which participates in inflammatory responses to contaminants (Moldoveanu et al., 2009). Activation of transcription factors and expression of pro-inflammatory genes are critical events in initiation of inflammation (Brown et al., 2001). Pro-inflammatory cytokines IL-6, IL-8 and IL-1β genes are up-regulated in AGS cells treated with polystyrene NPs of 44 nm and 100 nm at 10 μg/mL (Forte et al., 2016). Transcription of pro-inflammatory cytokines and inflammation-related cells factors, including IL-6, IL-8, NF-κb, and TNF-α genes, were up-regulated in A549 cells treated with polystyrene NPs of 25 nm at 25 μg/mL and 70 nm at 160 μg/mL (Xu et al., 2019). In the study results of which are presented here, genes associated with inflammation in A549 cells varied among treatments (Fig. 5). There was statistically significant up-regulation of expression of mRNA for IL-1β, IL-6, IL-8 and TNF-α genes in cells exposed to NPG-only, DBP-only, NPG+DBP, DEHP-only and NPG+DEHP, compared to the control. Expression of IL-6 and IL-8 genes were more responsive since their expressions in all exposures except for NPL-only, were more than twice that of control. Similar observation has been obtained that IL-6 and IL-8 genes showed more responsive changes in cells teared with polystyrene NPs (Forte et al., 2016). In addition, expressions of IL-1β, IL-6, IL-8 and TNF-α triggered by exposure to NPL+DBP or NPL+ DEHP were significantly down-regulated, but were up-regulated in cells exposed to NPG+DBP or NPG+DEHP, compared to respective DBP-only group and DEHP-only group. These inflammatory reactions might destroy integrities of A549 cell membranes and result in necrosis (Xu et al., 2019). It has been reported that when inhaled matter enters the respiratory system, in addition to ROS, to recruit inflammatory cells, cytokines are also secreted by airway epithelium (Moldoveanu et al., 2009). These local inflammatory responses can be amplified, giving rise to subsequent systemic inflammation and resulted in COPD and asthma. (Lodovici and Bigagli, 2011; MacNee, 2001).

When responses of A549, lung epithelial cells to combinations of PAEs and NPs were normalized to the control (Fig. 6), it was found that single exposure to NPs, DBP or DEHP all reduced viability of cells, initiated oxidative stress and inflammatory responses. When cells were co-exposed with the small concentration of NPs, cytotoxicity, oxidative stress, and inflammatory responses to PAEs were less due to lesser bioavailability, because of sorption to NPs. Due to its greater hydrophobicity and sorption capacity to NPs, this effect was greater for DEHP than DBP. Cytotoxicity, oxidative stress, and inflammatory responses of PAEs were greater when co-exposed with the greater concentration of NPs. Thus, exposure to NPs and properties of chemicals are crucial to determining responses to combined exposures of PAEs and NPs. Further research related to environmentally relevant plastic particles, combination with other contaminants and long-term effect studies are required for elucidating potential toxic effects due to the complexity of combined exposures (Koelmans et al., 2016; Shen et al., 2019).

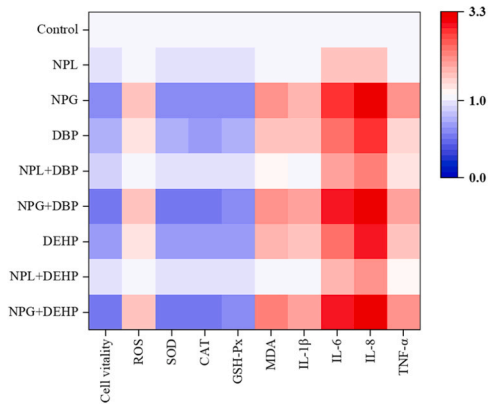

Fig. 6. Summary of responses of cells exposed to various treatments after normalization to the control group. control: control group; NPL: group exposed to 20 μg/mL polystyrene nanoplastics; NPG: group exposed to 200 μg/mL polystyrene nanoplastics; DBP: group exposed to 5 μg/mL dibutyl phthalate; NPL+DBP: group co-exposed to 20 μg/mL polystyrene nanoplastics and 5 μg/mL dibutyl phthalate; NPH+DBP: group co-exposed to 200 μg/mL polystyrene nanoplastics and 5 μg/mL dibutyl phthalate; DEHP: group exposed to 5 μg/mL di-(2-ethylhexyl) phthalate; NPL+DEHP: group co-exposed to 20 μg/mL polystyrene nanoplastics and 5 μg/mL di-(2-ethylhexyl) phthalate; NPH+DEHP: group co-exposed to 200 μg/mL polystyrene nanoplastics and 5 μg/mL di-(2-ethylhexyl) phthalate. ROS: reactive oxygen species; SOD: superoxide dismutase; CAT: catalase; GSH-Px: glutathione peroxidase; MDA: malondialdehyde; IL-1β: interleukin-1β; IL-6: interleukin-6; IL-8: interleukin-8; TNF-α: tumor necrosis factor-α.

4. Conclusions

The current study has confirmed the hypothesis that the A549 cells co-exposed to polystyrene NPs and PAEs (DEHP and DBP) exhibited changes in cell viability, oxidative stress and inflammatory reaction, and the combined toxic effects of NPs and PAEs on A549 cells were influenced by the exposure levels of NPs and properties of compounds. In combined exposure, the lesser concentration of NPs decreased the cell toxicity of both DBP and DEHP due to the reduction in bioavailability resulted from the sorption of PAEs to NPs, and there was a greater decrease in cytotoxicity in the combined exposure of DEHP than DBP because of the greater sorption capacity of DEHP to NPs. However, the greater concentration of NPs increased the cell toxicity of both DBP and DEHP since the dominant toxicity of high level of NPs during co-exposure. Therefore, this study provides the first detailed insight into the effect of NPs on the cytotoxicity of PAEs in A549 cells expanding our knowledge of the potential risk assessment of NPs and combined pollution on human health.

CRediT authorship contribution statement

Qingying Shi: Conceptualization, Methodology, Writing, Editing. **Jingchun Tang:** Conceptualization, Methodology, Reviewing, Editing. **Lan Wang:** Editing. **Rutao Liu:** Editing. **John P. Giesy:** Editing.

Declaration of Competing Interest

The authors declare that they have no known competing financial interests or personal relationships that could have appeared to influence the work reported in this paper.

Acknowledgments

The work was supported by National Natural Science Foundation of China [U1806216, 41807363], and 111 Program, Ministry of Education of China [T2017002]. Prof. Giesy was supported by the “High Level

Foreign Experts" program (#GDT20143200016) funded by the State Administration of Foreign Experts Affairs, the P.R. China to Nanjing University and the Einstein Professor Program of the Chinese Academy of Sciences. He was also supported by the Canada Research Chairs program and a Distinguished Visiting Professorship in the Department of Environmental Sciences at Baylor University, Waco, Texas, USA.

Appendix A. Supporting information

Supplementary data associated with this article can be found in the online version at doi:10.1016/j.ecoenv.2021.112041.

References

Ahamed, M., Akhtar, M.J., Khan, M.A.M., Alrokayan, S.A., Alhadlaq, H.A., 2019. Oxidative stress mediated cytotoxicity and apoptosis response of bismuth oxide (Bi2O3) nanoparticles in human breast cancer (MCF-7) cells. Chemosphere 216, 823–831.

Anand, K.V., Mohamed Jaabir, M.S., Thomas, P.A., Geraldine, P., 2012. Protective role of chrysin against oxidative stress in d-galactose-induced aging in an experimental rat model. Geriatr. Gerontol. Int. 12, 741–750.

Bakir, A., Rowland, S.J., Thompson, R.C., 2014. Enhanced desorption of persistent organic pollutants from microplastics under simulated physiological conditions. Environ. Pollut. 185, 16–23.

Baudrimont, M., Arini, A., Guégan, C., Venel, Z., Gigault, J., Pedrono, B., Prunier, J., Maurice, L., Ter Halle, A., Feurtet-Mazel, A., 2020. Ecotoxicity of polyethylene nanoplastics from the North Atlantic oceanic gyre on freshwater and marine organisms (microalgae and filter-feeding bivalves). Environ. Sci. Pollut. Res. 27, 3746–3755.

Benson, N.U., Fred-Ahmadu, O.H., 2020. Occurrence and distribution of microplastics-sorbed phthalic acid esters (PAEs) in coastal psammitic sediments of tropical Atlantic Ocean, Gulf of Guinea. Sci. Total Environ. 730, 139013.

Besseling, E., Wegner, A., Foekema, E.M., van den Heuvel-Greve, M.J., Koelmans, A.A., 2013. Effects of microplastic on fitness and PCB bioaccumulation by the lugworm Arenicola marina (L.). Environ. Sci. Technol. 47, 593–600.

Bhargava, S., et al., 2018. Fate of nanoplastics in marine larvae: a case study using barnacles Amphibalanus amphitrite. ACS Sustain. Chem. Eng. 6, 6932–6940.

Bouwmeester, H., Hollman, P.C.H., Peters, R.J.B., 2015. Potential health impact of environmentally released micro- and nanoplastics in the human food production chain: experiences from nanotoxicology. Environ. Sci. Technol. 49, 8932–8947.

Brown, D.M., Wilson, M.R., MacNee, W., Stone, V., Donaldson, K., 2001. Size-dependent proinflammatory effects of ultrafine polystyrene particles: a role for surface area and oxidative stress in the enhanced activity of ultrafines. Toxicol. Appl. Pharmacol. 175, 191–199.

Brun, N.R., van Hage, P., Hunting, E.R., Haramis, A.P.G., Vink, S.C., Vijver, M.G., Schaaf, M.J.M., Tudorache, C., 2019. Polystyrene nanoplastics disrupt glucose metabolism and cortisol levels with a possible link to behavioural changes in larval zebrafish. Commun. Biol. 2, 382, 382-382.

Chae, Y., An, Y.-J., 2017. Effects of micro- and nanoplastics on aquatic ecosystems: current research trends and perspectives. Mar. Pollut. Bull. 124, 624–632.

Chen, F.P., Chien, M.H., 2014. Lower concentrations of phthalates induce proliferation in human breast cancer cells. Climacteric 17, 377–384.

Chen, L., Zhang, J., Zhu, Y., Zhang, Y., 2018. Interaction of chromium(III) or chromium (VI) with catalase and its effect on the structure and function of catalase: an in vitro study. Food Chem. 244, 378–385.

Chiu, H.-W., Xia, T., Lee, Y.H., Chen, C.W., Tsai, J.C., Wang, Y.J., 2015. Cationic polystyrene nanospheres induce autophagic cell death through the induction of endoplasmic reticulum stress. Nanoscale 7, 736–746.

Clara, M., Windhofer, G., Hartl, W., Braun, K., Simon, M., Gans, O., Scheffknecht, C., Chovanec, A., 2010. Occurrence of phthalates in surface runoff, untreated and treated wastewater and fate during wastewater treatment. Chemosphere 78, 1078–1084.

Cortés, C., Domenech, J., Salazar, M., Pastor, S., Marcos, R., Hernández, A., 2020. Nanoplastics as a potential environmental health factor: effects of polystyrene nanoparticles on human intestinal epithelial Caco-2 cells. Environ. Sci. Nano 7, 272–285.

Cui, R., Kim, S.W., An, Y.J., 2017. Polystyrene nanoplastics inhibit reproduction and induce abnormal embryonic development in the freshwater crustacean Daphnia galeata. Sci. Rep. 7, 12095.

da Costa Araújo, A.P., Malafaia, G., 2021. Microplastic ingestion induces behavioral disorders in mice: a preliminary study on the trophic transfer effects via tadpoles and fish. J. Hazard. Mater. 401, 123263.

da Costa Araújo, A.P., de Melo, N.F.S., de Oliveira Junior, A.G., Rodrigues, F.P., Fernandes, T., de Andrade Vieira, J.E., Rocha, T.L., Malafaia, G., 2020. How much are microplastics harmful to the health of amphibians? A study with pristine polyethylene microplastics and Physalaemus cuvieri. J. Hazard. Mater. 382, 121066.

Dekkers, S., Krystek, P., Peters, R.J.B., Lankveld, D.P.K., Bokkers, B.G.H., van Hoeven-Arentzen, P.H., Bouwmeester, H., Oomen, A.G., 2011. Presence and risks of nanosilica in food products. Nanotoxicology 5, 393–405.

Della Torre, C., Bergami, E., Salvati, A., Faleri, C., Cirino, P., Dawson, K.A., Corsi, I., 2014. Accumulation and embryotoxicity of polystyrene nanoparticles at early stage of development of sea urchin embryos paracentrotus lividus. Environ. Sci. Technol. 48, 12302–12311.

Deville, S., Penjweini, R., Smisdom, N., Notelaers, K., Nelissen, I., Hooyberghs, J., Ameloot, M., 2015. Intracellular dynamics and fate of polystyrene nanoparticles in A549 Lung epithelial cells monitored by image (cross-) correlation spectroscopy and single particle tracking. Biochim. Biophys. Acta Mol. Cell Res. 1853, 2411–2419.

Ding, L., Mao, R., Ma, S., Guo, X., Zhu, L., 2020. High temperature depended on the ageing mechanism of microplastics under different environmental conditions and its effect on the distribution of organic pollutants. Water Res. 174, 115634.

Dong, C.-D., Chen, C.W., Chen, Y.C., Chen, H.H., Lee, J.S., Lin, C.H., 2020. Polystyrene microplastic particles: In vitro pulmonary toxicity assessment. J. Hazard. Mater. 385, 121575.

Dris, R., Gasperi, J., Mirande, C., Mandin, C., Guerrouache, M., Langlois, V., Tassin, B., 2017. A first overview of textile fibers, including microplastics, in indoor and outdoor environments. Environ. Pollut. 221, 453–458.

Erkekoğlu, P., Rachidi, W., De Rosa, V., Giray, B., Favier, A., Hıncal, F., 2010. Protective effect of selenium supplementation on the genotoxicity of di(2-ethylhexyl)phthalate and mono(2-ethylhexyl)phthalate treatment in LNCaP cells. Free Radic. Biol. Med. 49, 559–566.

Estrela, F.N., Batista Guimarães, A.T., Silva, F.G., Marinho da Luz, T., Silva, A.M., Pereira, P.S., Malafaia, G., 2021. Effects of polystyrene nanoplastics on Ctenopharyngodon idella (grass carp) after individual and combined exposure with zinc oxide nanoparticles. J. Hazard. Mater. 403, 123879.

Forte, M., Iachetta, G., Tussellino, M., Carotenuto, R., Prisco, M., De Falco, M., Laforgia, V., Valiante, S., 2016. Polystyrene nanoparticles internalization in human gastric adenocarcinoma cells. Toxicol. Vitr. 31, 126–136.

Fred-Ahmadu, O.H., Bhagwat, G., Oluyoye, I., Benson, N.U., Ayejuyo, O.O., Palanisami, T., 2020. Interaction of chemical contaminants with microplastics: principles and perspectives. Sci. Total Environ. 706, 135978.

Gao, M., Liu, Y., Song, Z., 2019. Effects of polyethylene microplastic on the phytotoxicity of di-n-butyl phthalate in lettuce (Lactuca sativa L. var. ramosa Hort). Chemosphere 237, 124482.

Guimarães, A.T.B., Estrela, F.N., Pereira, P.S., de Andrade Vieira, J.E., de Lima Rodrigues, A.S., Silva, F.G., Malafaia, G., 2021a. Toxicity of polystyrene nanoplastics in Ctenopharyngodon idella juveniles: a genotoxic, mutagenic and cytotoxic perspective. Sci. Total Environ. 752, 141937.

Guimarães, A.T.B., Estrela, F.N., Rodrigues, A.S.L., Chagas, T.Q., Pereira, P.S., Silva, F.G., Malafaia, G., 2021b. Nanopolystyrene particles at environmentally relevant concentrations causes behavioral and biochemical changes in juvenile grass carp (Ctenopharyngodon idella). J. Hazard. Mater. 403, 123864.

Huang, K., He, Y., Zhu, Z., Guo, J., Wang, G., Deng, C., Zhong, Z., 2019. Small, traceable, endosome-disrupting, and bioresponsive click nanogels fabricated via microfluidics for CD44-targeted cytoplasmic delivery of therapeutic proteins. ACS Appl. Mater. Interfaces 11, 22171–22180.

Kasahara, E., SATO, E.F., MIYOSHI, M., KONAKA, R., HIRAMOTO, K., SASAKI, J., TOKUDA, M., NAKANO, Y., INOUE, M., 2002. Role of oxidative stress in germ cell apoptosis induced by di(2-ethylhexyl)phthalate. Biochem. J. 365, 849–856.

Kim, H., Nam, K., Oh, S., Son, S., Jeon, D., Gye, M.C., Shin, I., 2019. Toxicological assessment of phthalates and their alternatives using human keratinocytes. Environ. Res. 175, 316–322.

Klaunig, J.E., Wang, Z., Pu, X., Zhou, S., 2011. Oxidative stress and oxidative damage in chemical carcinogenesis. Toxicol. Appl. Pharmacol. 254, 86–99.

Koelmans, A.A., Bakir, A., Burton, G.A., Janssen, C.R., 2016. Microplastic as a vector for chemicals in the aquatic environment: critical review and model-supported reinterpretation of empirical studies. Environ. Sci. Technol. 50, 3315–3326.

Kögel, T., Bjorøy, Ø., Toto, B., Bienfait, A.M., Sanden, M., 2020. Micro- and nanoplastic toxicity on aquatic life: determining factors. Sci. Total Environ. 709, 136050.

Langen, R.C.J., Korn, S.H., Wouters, E.F.M., 2003. ROS in the local and systemic pathogenesis of COPD. Free Radic. Biol. Med. 35, 226–235.

Lehner, R., Weder, C., Petri-Fink, A., Rothen-Rutishauser, B., 2019. Emergence of nanoplastic in the environment and possible impact on human health. Environ. Sci. Technol. 53, 1748–1765.

Li, Z., Yi, X., Zhou, H., Chi, T., Li, W., Yang, K., 2020a. Combined effect of polystyrene microplastics and dibutyl phthalate on the microalgae Chlorella pyrenoidosa. Environ. Pollut. 257, 113604.

Li, Z., Zhou, H., Liu, Y., Zhan, J., Li, W., Yang, K., Yi, X., 2020b. Acute and chronic combined effect of polystyrene microplastics and dibutyl phthalate on the marine copepod Tigriopus japonicus. Chemosphere 261, 127711.

Lim, S.L., Ng, C.T., Zou, L., Lu, Y., Chen, J., Bay, B.H., Shen, H.M., Ong, C.N., 2019. Targeted metabolomics reveals differential biological effects of nanoplastics and nanoZnO in human lung cells. Nanotoxicology 13, 1117–1132.

Lin, W., Jiang, R., Xiong, Y., Wu, J., Xu, J., Zheng, J., Zhu, F., Ouyang, G., 2019. Quantification of the combined toxic effect of polychlorinated biphenyls and nano-sized polystyrene on Daphnia magna. J. Hazard. Mater. 364, 531–536.

Liu, F., Liu, G., Zhu, Z., Wang, S., Zhao, F., 2019a. Interactions between microplastics and phthalate esters as affected by microplastics characteristics and solution chemistry. Chemosphere 214, 688–694.

Liu, L., Fokkink, R., Koelmans, A.A., 2016. Sorption of polycyclic aromatic hydrocarbons to polystyrene nanoplastic. Environ. Toxicol. Chem. 35, 1650–1655.

Liu, P., Lu, K., Li, J., Wu, X., Qian, L., Wang, M., Gao, S., 2020. Effect of aging on adsorption behavior of polystyrene microplastics for pharmaceuticals: adsorption mechanism and role of aging intermediates. J. Hazard. Mater. 384, 121193.

Liu, Y., Hu, Y., Yang, C., Chen, C., Huang, W., Dang, Z., 2019b. Aggregation kinetics of UV irradiated nanoplastics in aquatic environments. Water Res. 163, 114870.

Lodovici, M., Bigagli, E., 2011. Oxidative stress and air pollution exposure. J. Toxicol. 2011, 1–9, 487074-487074.

Lotfy, M.M., Hassan, H.M., Hetta, M.H., El-Gendy, A.O., Mohammed, R., 2018. Di-(2-ethylhexyl) Phthalate, a major bioactive metabolite with antimicrobial and cytotoxic activity isolated from River Nile derived fungus Aspergillus awamori. Beni Suef Univ. J. Basic Appl. Sci. 7, 263–269.
Lu, K., Qiao, R., An, H., Zhang, Y., 2018a. Influence of microplastics on the accumulation and chronic toxic effects of cadmium in zebrafish (Danio rerio). Chemosphere 202, 514–520.
Lu, S., Zhu, K., Song, W., Song, G., Chen, D., Hayat, T., Alharbi, N.S., Chen, C., Sun, Y., 2018b. Impact of water chemistry on surface charge and aggregation of polystyrene microspheres suspensions. Sci. Total Environ. 630, 951–959.
MacNee, W., 2001. Oxidative stress and lung inflammation in airways disease. Eur. J. Pharmacol. 429, 195–207.
Manfra, L., Rotini, A., Bergami, E., Grassi, G., Faleri, C., Corsi, I., 2017. Comparative ecotoxicity of polystyrene nanoparticles in natural seawater and reconstituted seawater using the rotifer Brachionus plicatilis. Ecotoxicol. Environ. Saf. 145, 557–563.
Mao, R., Lang, M., Yu, X., Wu, R., Yang, X., Guo, X., 2020. Aging mechanism of microplastics with UV irradiation and its effects on the adsorption of heavy metals. J. Hazard. Mater. 393, 122515.
Mato, Y., Isobe, T., Takada, H., Kanehiro, H., Ohtake, C., Kaminuma, T., 2001. Plastic resin pellets as a transport medium for toxic chemicals in the marine environment. Environ. Sci. Technol. 35, 318–324.
Meindl, C., Kueznik, T., Bösch, M., Roblegg, E., Fröhlich, E., 2015. Intracellular calcium levels as screening tool for nanoparticle toxicity. J. Appl. Toxicol. 35, 1150–1159.
Moldoveanu, B., et al., 2009. Inflammatory mechanisms in the lung. J. Inflamm. Res. 2, 1–11.
Molino, C., Filippi, S., Stoppiello, G.A., Meschini, R., Angeletti, D., 2019. In vitro evaluation of cytotoxic and genotoxic effects of Di(2-ethylhexyl)-phthalate (DEHP) on European sea bass (Dicentrarchus labrax) embryonic cell line. Toxicol. Vitr. 56, 118–125.
Müller, J., Kördel, W., 1993. Occurrence and fate of phthalates in soil and plants. Sci. Total Environ. 134, 431–437.
Nolte, T.M., Hartmann, N.B., Kleijn, J.M., Garnæs, J., van de Meent, D., Jan Hendriks, A., Baun, A., 2017. The toxicity of plastic nanoparticles to green algae as influenced by surface modification, medium hardness and cellular adsorption. Aquat. Toxicol. 183, 11–20.
de Oliveira, J.P.J., Estrela, F.N., Rodrigues, A.S.L., Guimarães, A.T.B., Rocha, T.L., Malafaia, G., 2021. Behavioral and biochemical consequences of Danio rerio larvae exposure to polylactic acid bioplastic. J. Hazard. Mater. 404, 124152.
Pandey, S., PARVEZ, S., SAYEED, I., HAQUE, R., BINHAFEEZ, B., RAISUDDIN, S., 2003. Biomarkers of oxidative stress: a comparative study of river Yamuna fish Wallago attu (Bl. & Schn.). Sci. Total Environ. 309, 105–115.
Peropadre, A., 2013. Cytotoxic effects of di (2-ethylhexyl) phthalate on cultured mammalian cells. Curr. Top. Toxicol. 9, 35–42.
Peropadre, A., Fernández Freire, P., Pérez Martín, J.M., Herrero, Ó., Hazen, M.J., 2015. Endoplasmic reticulum stress as a novel cellular response to di (2-ethylhexyl) phthalate exposure. Toxicol. Vitr. 30, 281–287.
Poma, A., Vecchiotti, G., Colafarina, S., Zarivi, O., Aloisi, M., Arrizza, L., Chichiriccò, G., Di Carlo, P., 2019. In vitro genotoxicity of polystyrene nanoparticles on the human fibroblast Hs27 cell line. Nanomaterials 9, 1299.
Prata, J.C., da Costa, J.P., Lopes, I., Duarte, A.C., Rocha-Santos, T., 2020. Environmental exposure to microplastics: an overview on possible human health effects. Sci. Total Environ. 702, 134455.
Prietl, B., Meindl, C., Roblegg, E., Pieber, T.R., Lanzer, G., Fröhlich, E., 2014. Nano-sized and micro-sized polystyrene particles affect phagocyte function. Cell Biol. Toxicol. 30, 1–16.
Rengel, R.G., Filipović-Grčić, J., Čepelak, I., Žanić-Grubišić, T., Barišić, K., 2005. The effect of liposomes with superoxide dismutase on A2182 cells. Eur. J. Pharm. Biopharm. 60, 47–51.
Rios Mendoza, L.M., Karapanagioti, H., Álvarez, N.R., 2018. Micro(nanoplastics) in the marine environment: current knowledge and gaps. Curr. Opin. Environ. Sci. Health 1, 47–51.
Rodrigues, J.P., Duarte, A.C., Santos-Echeandía, J., Rocha-Santos, T., 2019. Significance of interactions between microplastics and POPs in the marine environment: a critical overview. TrAC Trends Anal. Chem. 111, 252–260.
Ruenraroengsak, P., Tetley, T.D., 2015. Differential bioreactivity of neutral, cationic and anionic polystyrene nanoparticles with cells from the human alveolar compartment: robust response of alveolar type 1 epithelial cells. Part. Fibre Toxicol. 12, 19.
Ruenraroengsak, P., Novak, P., Berhanu, D., Thorley, A.J., Valsami-Jones, E., Gorelik, J., Korchev, Y.E., Tetley, T.D., 2012. Respiratory epithelial cytotoxicity and membrane damage (holes) caused by amine-modified nanoparticles. Nanotoxicology 6, 94–108.
Schirinzi, G.F., Pérez-Pomeda, I., Sanchís, J., Rossini, C., Farré, M., Barceló, D., 2017. Cytotoxic effects of commonly used nanomaterials and microplastics on cerebral and epithelial human cells. Environ. Res. 159, 579–587.
Schönlau, C., Larsson, M., Lam, M.M., Engwall, M., Giesy, J.P., Rochman, C., Kärrman, A., 2019. Aryl hydrocarbon receptor-mediated potencies in field-deployed plastics vary by type of polymer. Environ. Sci. Pollut. Res. 26, 9079–9088.
Shen, M., Zhang, Y., Zhu, Y., Song, B., Zeng, G., Hu, D., Wen, X., Ren, X., 2019. Recent advances in toxicological research of nanoplastics in the environment: a review. Environ. Pollut. 252, 511–521.
Shi, C., Wang, Q., Liao, X., Ge, H., Huo, G., Zhang, L., Chen, N., Zhai, X., Hong, Y., Wang, L., Han, Y., Xiao, W., Wang, Z., Shi, W., Mao, Y., Yu, J., Xia, G., Liu, Y., 2019a. Discovery of 6-(2-(dimethylamino)ethyl)-N-(5-fluoro-4-(4-fluoro-1-isopropyl-2-methyl- 1H-benzo d imidazole-6-yl)pyrimidin-2-yl)-5,6,7,8-tetrahydro-1,6-naphthyridin-2-amine as a highly potent cyclin-dependent kinase 4/6 inhibitor for treatment of cancer. Eur. J. Med. Chem. 178, 352–364.
Shi, Q., Luo, X., Huang, Z., Midgley, A.C., Wang, B., Liu, R., Zhi, D., Wei, T., Zhou, X., Qiao, M., Zhang, J., Kong, D., Wang, K., 2019b. Cobalt-mediated multi-functional dressings promote bacteria-infected wound healing. Acta Biomater. 86, 465–479.
Sørensen, L., Rogers, E., Altin, D., Salaberria, I., Booth, A.M., 2020. Sorption of PAHs to microplastic and their bioavailability and toxicity to marine copepods under co-exposure conditions. Environ. Pollut. 258, 113844.
Sun, X., Chen, B., Li, Q., Liu, N., Xia, B., Zhu, L., Qu, K., 2018. Toxicities of polystyrene nano- and microplastics toward marine bacterium Halomonas alkaliphila. Sci. Total Environ. 642, 1378–1385.
Teil, M.J., Blanchard, M., Chevreuil, M., 2006. Atmospheric fate of phthalate esters in an urban area (Paris-France). Sci. Total Environ. 354, 212–223.
Tourinho, P.S., Kočí, V., Loureiro, S., van Gestel, C.A.M., 2019. Partitioning of chemical contaminants to microplastics: Sorption mechanisms, environmental distribution and effects on toxicity and bioaccumulation. Environ. Pollut. 252, 1246–1256.
Tousoulis, D., Andreou, I., Antoniades, C., Tentolouris, C., Stefanadis, C., 2008. Role of inflammation and oxidative stress in endothelial progenitor cell function and mobilization: therapeutic implications for cardiovascular diseases. Atherosclerosis 201, 236–247.
Trevisan, R., Voy, C., Chen, S., Di Giulio, R.T., 2019. Nanoplastics decrease the toxicity of a complex PAH mixture but impair mitochondrial energy production in developing zebrafish. Environ. Sci. Technol. 53, 8405–8415.
Wang, C., Nie, G., Yang, F., Chen, J., Zhuang, Y., Dai, X., Liao, Z., Yang, Z., Cao, H., Xing, C., Hu, G., Zhang, C., 2020a. Molybdenum and cadmium co-induce oxidative stress and apoptosis through mitochondria-mediated pathway in duck renal tubular epithelial cells. J. Hazard. Mater. 383, 121157.
Wang, J., Liu, X., Liu, G., 2019. Sorption behaviors of phenanthrene, nitrobenzene, and naphthalene on mesoplastics and microplastics. Environ. Sci. Pollut. Res. 26, 12563–12573.
Wang, Q., Bai, J., Ning, B., Fan, L., Sun, T., Fang, Y., Wu, J., Li, S., Duan, C., Zhang, Y., Liang, J., Gao, Z., 2020b. Effects of bisphenol A and nanoscale and microscale polystyrene plastic exposure on particle uptake and toxicity in human Caco-2 cells. Chemosphere 254, 126788.
Wright, S.L., Thompson, R.C., Galloway, T.S., 2013. The physical impacts of microplastics on marine organisms: a review. Environ. Pollut. 178, 483–492.
Wu, B., Wu, X., Liu, S., Wang, Z., Chen, L., 2019. Size-dependent effects of polystyrene microplastics on cytotoxicity and efflux pump inhibition in human Caco-2 cells. Chemosphere 221, 333–341.
Wu, Q., Lam, J.C.W., Kwok, K.Y., Tsui, M.M.P., Lam, P.K.S., 2017. Occurrence and fate of endogenous steroid hormones, alkylphenol ethoxylates, bisphenol A and phthalates in municipal sewage treatment systems. J. Environ. Sci. 61, 49–58.
Xia, T., Kovochich, M., Liong, M., Zink, J.I., Nel, A.E., 2008. Cationic polystyrene nanosphere toxicity depends on cell-specific endocytic and mitochondrial injury pathways. ACS Nano 2, 85–96.
Xu, M., Halimu, G., Zhang, Q., Song, Y., Fu, X., Li, Y., Li, Y., Zhang, H., 2019. Internalization and toxicity: a preliminary study of effects of nanoplastic particles on human lung epithelial cell. Sci. Total Environ. 694, 133794.
Yu, X., Hong, S., Moreira, E.G., Faustman, E.M., 2009. Improving in vitro Sertoli cell/gonocyte co-culture model for assessing male reproductive toxicity: lessons learned from comparisons of cytotoxicity versus genomic responses to phthalates. Toxicol. Appl. Pharmacol. 239, 325–336.
Zhang, S., Ding, J., Razanajatovo, R.M., Jiang, H., Zou, H., Zhu, W., 2019a. Interactive effects of polystyrene microplastics and roxithromycin on bioaccumulation and biochemical status in the freshwater fish red tilapia (Oreochromis niloticus). Sci. Total Environ. 648, 1431–1439.
Zhang, S., Zhang, J., Chen, H., Wang, A., Liu, Y., Hou, H., Hu, Q., 2019b. Combined cytotoxicity of co-exposure to aldehyde mixtures on human bronchial epithelial BEAS-2B cells. Environ. Pollut. 250, 650–661.
Zhang, W., Liu, Z., Tang, S., Li, D., Jiang, Q., Zhang, T., 2020. Transcriptional response provides insights into the effect of chronic polystyrene nanoplastic exposure on Daphnia pulex. Chemosphere 238, 124563.
Zhao, Y., Ao, H., Chen, L., Sottas, C.M., Ge, R., Li, L., Zhang, Y., 2012. Mono-(2-ethylhexyl) phthalate affects the steroidogenesis in rat Leydig cells through provoking ROS perturbation. Toxicol. Vitr. 26, 950–955.
Zhou, Q., Yue, Z., Li, Q., Zhou, R., Liu, L., 2019. Exposure to PbSe nanoparticles and male reproductive damage in a rat model. Environ. Sci. Technol. 53, 13408–13416.
Zhu, J., Kovacs, L., Han, W., Liu, G., Huo, Y., Lucas, R., Fulton, D., Greer, P.A., Su, Y., 2019. Reactive oxygen species-dependent calpain activation contributes to airway and pulmonary vascular remodeling in chronic obstructive pulmonary disease. Antioxid. Redox Signal. 31, 804–818.
Zuo, L., Hallman, A.H., Roberts, W.J., Wagner, P.D., Hogan, M.C., 2014. Superoxide release from contracting skeletal muscle in pulmonary TNF-alpha overexpression mice. Am. J. Physiol. Regul. Integr. Comp. Physiol. 306, R75–R81.

Supplementary Information for

Combined cytotoxicity of polystyrene nanoplastics and phthalate esters on human lung epithelial A549 cells and its mechanism

Qingying Shi[a], Jingchun Tang[a,*], Lan Wang[a], Rutao Liu[b], John P. Giesy[c, d, e]

[a]Key Laboratory of Pollution Processes and Environmental Criteria (Ministry of Education), Tianjin Engineering Center of Environmental Diagnosis and Contamination Remediation, College of Environmental Science and Engineering, Nankai University, Tianjin 300350, China.

[b]School of Environmental Science and Engineering, Shandong University, China-America CRC for Environment & Health, 72# Jimo Binhai Road, Qingdao, Shandong, 266237, PR China

[c]Toxicology Centre, University of Saskatchewan, 44 Campus Drive, Saskatoon SK S7N 5B3, Canada

[d]Dept. Veterinary Biomedical Sciences, University of Saskatchewan, 52 Campus Drive, Saskatoon, SK S7N 5B4, Canada

[e]Dept. Environmental Sciences, Baylor University, Waco, TX, USA, 76798-7266

*Corresponding Authors: Jingchun Tang, E-mail: tangjch@nankai.edu.cn

Number of Pages: 11

Number of Figures: 3

Number of Tables: 4

Additional Details on Materials and Methods

Text S1

The quantification of NPs was performed according to previous study (Estrela et al., 2021), with some modifications. After the 24-hours exposure of different treatments to A549 cells cultured in tissue culture plates, the supernatants were collected and washed for three times for the quantification of NPs in the cell culture medium that did not enter the cells. In addition, the cells were collected and homogenized with PBS to detect the NPs accumulated in cells. Next, 100 μL of each sample was added to the microplate wells (in triplicate) and the fluorescent intensities were measured on a microplate reader (Synergy H4, Bio-Tek, Vermont, USA). The quantification of NPs was calculated based on the standard curve plotted from NPs suspensions at eight different standard concentrations. The background luminescence of cells that were not exposed to NPs was detected and subtracted from that of NPs-exposed samples. The estimated concentrations of NPs in cell culture medium were expressed in μg/mL and the accumulation of NPs in cells were expressed in ng/10^3 cells.

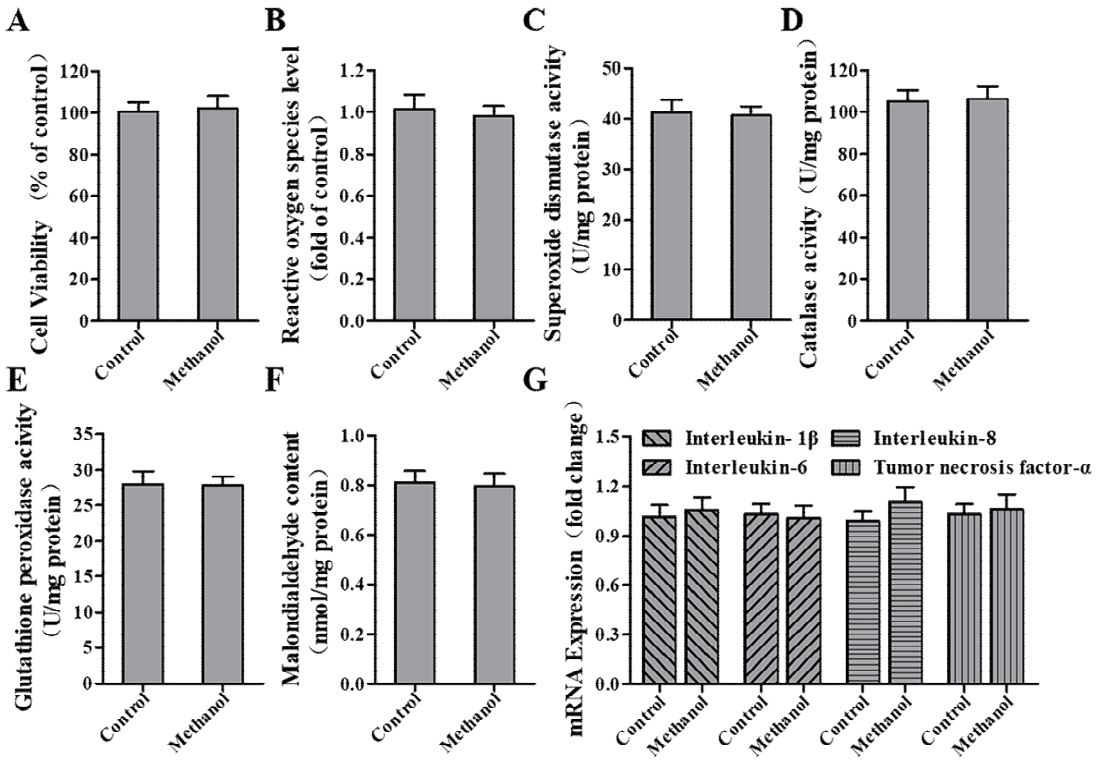

Fig S1. Effects of solvent methanol on A549 cells. (A) Viability of A549 cells; t = 0.2120, p = 0.8425; (B) Effect of methanol on intercellular reactive oxygen species in A549 cells; t = 0.6548, p = 0.5483; (C) Effect of co-exposure of NPs and PAEs on the activity of superoxide dismutase; t = 0.1637, p = 0.8779; (D) Effect of methanol on the activity of catalase; t = 0.08491, p = 0.9364; (E) Effect of methanol on the activity of glutathione peroxidase; t = 0.04053, p = 0.9696; (F) Effect of methanol on the content of malondialdehyde; t = 0.2638, p = 0.8050; (G) Effects of methanol on expressions of mRNA fo interleukin-1β (t = 0.3605, p = 0.7367), interleukin-6 (t = 0.2159, p = 0.8396), interleukin-8 (t = 0.4157, p = 0.9070) and tumor necrosis factor-α (t = 0.2357, p = 0.8252). Control: control group; Methanol: group exposed to 0.01% methanol.

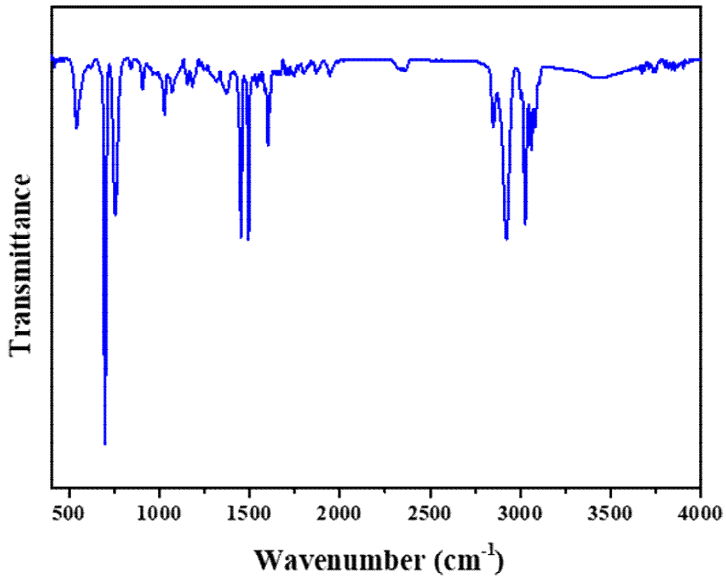

Fig S2. Fourier transform infrared spectroscopy spectrum of NPs used in this study.

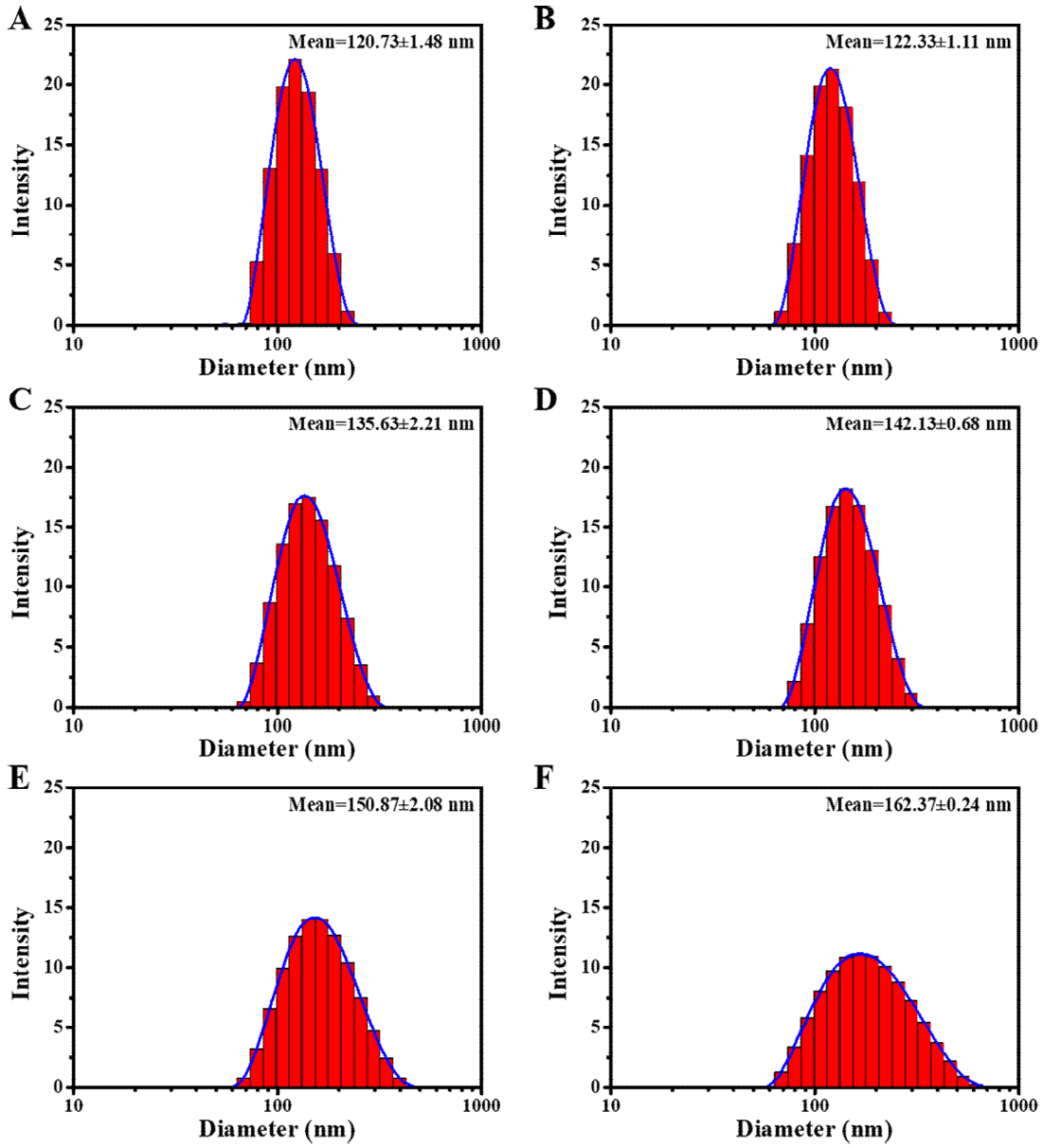

Fig S3. Distribution of sizes of NPs after combined exposure at 24 hours tested by dynamic light scattering. (A) Size distribution of NPs in group exposed to 20 μg/mL polystyrene nanoplastics; (B) Size distribution of NPs in group exposed to 200 μg/mL polystyrene nanoplastics; (C) Size distribution of NPs in group co-exposed to 20 μg/mL polystyrene nanoplastics and 5 μg/mL dibutyl phthalate; (D) Size distribution of NPs in group co-exposed to 200 μg/mL polystyrene nanoplastics and 5 μg/mL dibutyl phthalate; (E) Size distribution of NPs in group co-exposed to 20 μg/mL polystyrene nanoplastics and 5 μg/mL di-(2-ethylhexyl) phthalate; (F) Size distribution of NPs in

group co-exposed to 200 μg/mL polystyrene nanoplastics and 5 μg/mL di-(2-ethylhexyl) phthalate.

Table S1. Physical-chemical properties of selected phthalate esters.

PAEs	CAS	molecular formula	molar mass (g/mol)	density (g/cm^3)	logK_{ow} (Pérez-Albaladejo et al., 2017)	solubility (mg/L) (Pérez-Albaladejo et al., 2017)
DBP	84-74-2	$C_{16}H_{22}O_4$	278.34	1.05	4.1	11.10
DEHP	117-81-7	$C_{24}H_{38}O_4$	390.56	0.98	7.3	0.39

PAEs: phthalate esters; DBP: dibutyl phthalate; DEHP: di-(2-ethylhexyl) phthalate.

Table S2. Primers used in quantitative real-time PCR.

Gene	Forward primer	Reverse primer
IL-1β	ACGATGCACCTGTACGATCACT	CACCAAGCTTTTTTGCTGTGAG
IL-6	TTCCAAAGATGTAGCCGCCC	GTTGGGTCAGGGGTGGTTATT
IL-8	CATACTCCAAACCTTTCCACC	AAACTTCTCCACAACCCTCTG
TNF-α	CCCAGGGACCTCTCTCTAATCA	AGCTGCCCCTCAGCTTGAG
GAPDH	TGGTATCGTGGAAGGACTCA	CCAGTAGAGGCAGGGATGAT

IL-1β: interleukin-1β; IL-6: interleukin-6; IL-8: interleukin-8; TNF-α: tumor necrosis factor-α; GAPDH: glyceraldehyde phosphate dehydrogenase.

Table S3. Physical characteristics of NPs.

	Hydrodynamic diameter (nm)	Polydispersity index	Zeta potential (mV)
Ultrapure water	104.77±1.47	0.027±0.001	-16.30±1.07
Cell medium	117.23±1.96	0.051±0.010	-4.77±1.02

Table S4. The quantification of NPs in cell culture medium and in cells in different treatment groups.

	Nominal concentrations of NPs (μg/mL)	Nominal concentration of PAEs (μg/mL)	Concentrations of NPs in cell culture medium (μg/mL)	Accumulation of NPs in cells (ng/10^3 cells)
Control	0	0	n.d.	n.d.
NPL	20	0	16.03±1.23	6.01±0.08
NPG	200	0	156.68±9.49	64.98±4.23
DBP	0	5	n.d.	n.d.
NPL+DBP	20	5	16.07±1.66	5.89±0.05
NPG+DBP	200	5	158.66±12.18	63.51±5.03
DEHP	0	5	n.d.	n.d.
NPL+DEHP	20	5	16.14±0.75	5.72±0.18
NPG+DEHP	200	5	158.99±9.72	62.79±1.12

n.d.: not detected. Numerical data represent the mean ± standard deviation. PAEs: phthalate esters. control: control group; NPL: group exposed to 20 μg/mL polystyrene nanoplastics; NPG: group exposed to 200 μg/mL polystyrene nanoplastics; DBP: group exposed to 5 μg/mL dibutyl phthalate; NPL+DBP: group co-exposed to 20 μg/mL polystyrene nanoplastics and 5 μg/mL dibutyl phthalate; NPH+DBP: group co-exposed to 200 μg/mL polystyrene nanoplastics and 5 μg/mL dibutyl phthalate; DEHP: group exposed to 5 μg/mL di-(2-ethylhexyl) phthalate; NPL+DEHP: group co-exposed to 20 μg/mL polystyrene nanoplastics and 5 μg/mL di-(2-ethylhexyl) phthalate; NPH+DEHP: group co-exposed to 200 μg/mL polystyrene nanoplastics and 5 μg/mL di-(2-ethylhexyl) phthalate.

Reference

Estrela, F. N., et al., 2021. Effects of polystyrene nanoplastics on Ctenopharyngodon idella (grass carp) after individual and combined exposure with zinc oxide nanoparticles. Journal of Hazardous Materials. 403**,** 123879.

Pérez-Albaladejo, E., et al., 2017. Comparative toxicity, oxidative stress and endocrine disruption potential of plasticizers in JEG-3 human placental cells. Toxicology in Vitro. 38**,** 41-48.